PCCP

Accepted Manuscript

ROYAL SOCIETY OF CHEMISTRY

www.rsc.org/pccp

PCCP

RSCPublishing

ARTICLE

Novel 2-Alkyl-1-Ethylpyridinium Ionic Liquids: Synthesis, Dissociation Energies and Volatility

Cite this: DOI: 10.1039/x0xx00000x

Miguel Vilas [a], Marisa A. A. Rocha [b,1], Ana M. Fernandes [c], Emilia Tojo[*,a], Luís M. N. B. F. Santos[*,b]

Received 00th January 2012,
Accepted 00th January 2012

DOI: 10.1039/x0xx00000x

www.rsc.org/

This work presents the synthesis, volatility study and electrospray tandem mass spectrometry with variable collision induced of the isolated [(cation)$_2$(anion)]+ of a novel series of 2-alkyl-1-ethyl pyridinium based ionic liquids, [$^2C_{N-2}{}^1C_2Py$][NTf_2]. Compared to the imidazolium based ionic liquids, the new ionic liquid series presents a higher thermal stability and lower volatility. The [(cation)$_2$(anion)]+ collision induced dissociation energies of both [$^2C_{N-2}{}^1C_2Py$][NTf_2] and [C_NPy][NTf_2] pyridinium series, show an identical trend with a pronounced decrease of the relative cation-anion interaction energy towards an almost constant value for N=6. It was found that the lower volatility of the [$^2C_{N-2}{}^1C_2Py$][NTf_2] with shorter alkyl chain length, is due to their higher enthalpies of vaporization. Starting from [$^2C_3{}^1C_2Py$][NTf_2], the lower volatility is ruled by the combination of slightly lower entropies and higher enthalpies of vaporization, being an indication of a higher structural disorder of the pyridinium based ionic liquids than the imidazolium based ionic liquids. Dissociation energies and volatility trends supports the cohesive energy interpretation model based in the overlapping the electrostatic and van der Waals functional interaction potentials.

Introduction

The understanding of the physical chemical properties of ionic liquids (ILs) hinges on the proper comprehension of the molecular structure of the compounds in the liquid phase. It is well accepted nowadays that ionic liquids are highly structured fluids. The long-range structuration of ionic liquids was studied by Urahata and Ribeiro,[1] using computer simulation to provide a perspective view of the ionic motions and the onset of distinct dynamical processes in ionic liquids. Later, Wang and Voth[2] explored the effect of the alkyl side chain length of the cation in ionic liquids, using a multiscale coarse-graining (MS-CG) method.[2,3] Based on this work, it was found for extended lengths of the alkyl chains, that the tail groups of the cations aggregate to form spatial heterogeneous tail domains, where the head groups and the anions distribute reasonably homogeneous in order to maintain electroneutrality as well as to maximize the electrostatic interactions, while the tail groups tend to segregate elsewhere.[2] In 2006, for the first time, Lopes and Pádua[4] used atomistic simulation to study the nanostructuration of 1-alkyl-3-methylimidazolium based ionic liquids, [$C_{N-1}C_1im$]$^+$ (N = 3 up to 13), in the liquid phase, and to investigate the effect of the alkyl side chain length of the cations on the long-range structures. Based on this work it was possible to predict that the structure of the liquid phase of the studied ionic liquids exhibits microphase separation between polar and nonpolar regions. Additionally, it was observed that the polar regions has the structure of a tridimensional network of ionic channels, while the nonpolar regions are arranged as dispersed microphases, for the [C_2C_1im]$^+$ based ILs, and as a continuous phase for higher alkyl chains lengths.[5] The interaction between these two types of regions (polar and nonpolar) led to the recognition of ionic liquids as high-charge density (polar) networks permeated by low-charge density (nonpolar) regions.[1–6] This characteristic of the structural organization of ionic liquids was first experimentally supported by X-ray diffraction[7] and later by small-wide angle X-ray scattering (SWAXS).[8,9] Neutron diffraction was used to study the structures of 1,3-dimethylimidazolium chloride,[10] [C_1C_1im][Cl], and hexafluorophosphate,[11] [C_1C_1im][PF_6], ionic liquids. The comparison of diffraction patterns of deuterated and protonated liquids enable a detailed picture of the anion-cation and cation-cation interactions. Based on this work, a high charge ordering with similar anion-cation interactions for both anions was found. In both works, a strong correlation between the solid and liquid phases was detected. It was also observed that the degree of charge ordering becomes less pronounced for large anions and asymmetrical cations.[10–13] Recently, a combination of infrared (IR) spectroscopic techniques was used to characterize the degree of charge organization present in the

a Department of Organic Chemistry, University of Vigo, Faculty of Chemistry, Marcosende, Vigo, Spain
E-mail: etojo@uvigo.es
b CIQ, Departamento de Química e Bioquímica, Faculdade de Ciências da Universidade do Porto, Porto, Portugal
E-mail: lbsantos@fc.up.pt
c QOPNA Unit, Departamento de Química, Universidade de Aveiro, 3810-193 Aveiro, Portugal
[1] Current address: Department of Chemical Engineering and Chemistry, Eindhoven University of Technology, Eindhoven, The Netherlands.

imidazolium based ionic liquids family.[14] It was found that longer alkyl side chains attached onto the imidazolium ions increases the short-range repulsive interactions among the ions and disrupt the charge organization, in agreement with previous studies.[7,15] Recently, a comprehensive molecular dynamics simulation study has been performed in order to complement and extend the structural analysis on the mesoscopic segregation observed in the ionic liquids of the 1-alkyl-3-methylimidazolium bis(trifluoromethylsulfonyl)imide, $[C_{N-1}C_1im][NTf_2]$.[16] It was found that in the smaller members (C2 – C4) of the ionic liquid series, the non-polar aggregates form elongated clusters with an increasing number of tails per aggregate, that become more oblate around $[C_5C_1im][NTf_2]$ and starting from $[C_6C_1im][NTf_2]$ forms a second continuous sub-phase.[16]

The possibility of concisely tuning the physical chemical properties by changing the cation-anion combination is one of the biggest advantages of these systems. For this purpose, the knowledge and understanding of structure−property relationships of ionic liquids is indispensable.[17,18] Therefore, great efforts have been made in order to determine these properties experimentally or by theoretical calculations.[17–25] Due to the large number of possible ionic liquids, predictive models have been proposed to overcome this limitation.[26–30] Until recently, ionic liquids were regarded as non-volatile, and thus did not exhibit measurable vapor pressures, even at higher temperatures. However, Earle *et al.*[29] have shown that some ionic liquids can be distilled at low pressures without decomposition. Later on, Paulechka *et al.*[31] have evaluated the possibility of measuring the vapor pressure and enthalpy of vaporization of $[C_4C_1im][NTf_2]$ in vacuum. Kabo and collaborators [32] reported the first experimental determinations of vapor pressures for a series of $[C_{N-1}C_1im][NTf_2]$ (N = 3, 5, 7, and 9) ionic liquids, using an integral Knudsen effusion method. It was shown that the balance of the thermal stability and volatility for $[C_{N-1}C_1im][NTf_2]$ allowed measurements of vapor pressures in a temperature range suitable for a proper evaluation of the thermodynamic properties of vaporization. The nature of the gas phase of ionic liquids is still in debate, however the theory that the vaporization of ionic liquids occurs as a direct liquid to gas transfer of the intact ionic pair, has been supported by studies using calorimetry[33], photoionization,[34] line of sight mass spectrometry,[35–37] Fourier transform ion cyclotron resonance [38,39], and by tunable vacuum ultraviolet photoionization [40]. These pioneering works [31–40] contributed to the knowledge of a window of opportunity [19] for the vaporization of some ionic liquids without decomposition. In addition to the already cited works concerning the vapor pressure measurements by the integral Knudsen effusion method [32] and the determination of enthalpies of vaporization by Calvet drop microcalorimetry [33], several other techniques and strategies were used to determine the enthalpies of vaporization. Nowadays, there are a number of publications reporting enthalpies of vaporization, at a reference temperature, for a wide range of ionic liquids determined using both experimental [35,36,40–46] and theoretical methods.[47,48]

Accurate thermodynamic properties of vaporization equilibrium of ionic liquids are scarce and fundamental for the better understanding of the liquid phase of ionic liquids, evaluation of the cohesive energy, as well as the nature of the vapor phase. Additionally, they are required for validation and parameterization of the models (force fields) used to describe ionic liquids in different simulation techniques.[3,6,19,49] Despite of the importance of the vapor pressures of ionic liquids and the related thermodynamic properties of vaporization, $\Delta_l^g H_m^o$, $\Delta_l^g S_m^o$, and $\Delta_l^g G_m^o$, respectively, most of the works are focused on the estimation and determination of enthalpies of vaporization.[19] Our group has been focused on the vapor pressure measurements of several families of ionic liquids,[50–55] using the quartz microbalance Knudsen effusion apparatus.[56] In these works, the effect of the alkyl chain length of the cation was explored in order to get more insights about the nanostructuration of ionic liquids, which is related with the transition from a dispersed to a continuous non-polar phase, as the alkyl-side chain of the cation becomes longer.[5] It was possible to give a thermodynamic view of the nanostructuration of the imidazolium bistriflamide ionic liquids, for which a limit for the beginning of the nanostructuration / nano segregation at C_6 was observed.[50,55,57] Recently, the first volatility study of the 1-alkylpyridinium bis(trifluoromethylsulfonyl)imide, $[C_NPy][NTf_2]$ (N= 2, 3, and 4) was reported, and the analysis and rationalization of the obtained results was done based on the comparison with the series $[C_{N-1}C_1im][NTf_2]$ (N= 3 − 5).[50,51] It was found that the volatility of pyridinium ionic liquids is five times lower than that of imidazolium and that it is driven by their higher enthalpy of vaporization.[53]

Imidazolium based ionic liquids are the most investigated family in several research areas. Compared to the imidazolium cation, the pyridinium cation have lower cost, low toxicity, chemical stability and a high extractive performance.[58–61] The change of the cation from a imidazolium to a pyridinium leads to a different kind of structural organization in the liquid phase, and the enlargement of the cation size increases the distance between charges while delocalizing them as well, thus resulting in a decrease in the ionic interaction energy.[62,63] Despite the decrease of the electrostatic interactions, the pyridinium based ionic liquids have found to be associated with a higher cohesion than the imidazolium ionic liquids, which is associated to the importance of cation-cation dispersive interactions.[64,65] The molecular interactions between the ions and their structural arrangement results in a complex structural / nanostructural organization and hence to interesting properties. Therefore, the knowledge of the dependence ionic liquids properties on their molecular structures is of great importance.

The present work comprises the synthesis and volatility study of a novel series of 2-alkyl-1-ethylpyridinium bis(trifluoromethane sulfonyl)imide, $[^2C_{N-2}{}^1C_2Py][NTf_2]$ (N = 4 − 12), ionic liquids. The inspiration for the design of this novel pyridinium based ionic liquids series was based on the idea of mimics the properties and thermal stability of the dialkylimidazolium base ILs, in a different chemical moiety that presents some applicability advantages.[58–61] The vapor pressure of each pure ionic liquid was determined as a function of temperature in the [493 − 535] K range, using a new quartz microbalance Knudsen effusion apparatus.[55] Based on the experimental results, the standard molar enthalpy, entropy and Gibbs energy of vaporization were obtained. Electrospray ionization mass spectrometry data were further used to gather additional insights into the interpretation of the thermodynamic properties of vaporization in terms of the IL's interaction energies. In this work, by means of a comparative analysis with previous studies,[50] the effect of nanostructuration on the pyridinium bistriflamide ionic liquids was explored.

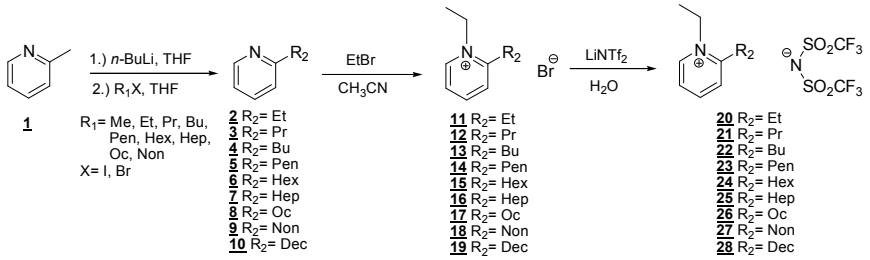

Scheme 1. General synthetic procedure employed to prepare the new 2-alkyl-1-ethylpyridinium ILs.

Results and Discussion

Synthesis: The new 1-ethyl-2-alkylpyridinium ionic liquids were synthesized in a three-step process following the general route shown in Scheme 1. The introduction of different alkyl groups in position 2 of the pyridine ring was carried out by metalation of commercial 2-picoline (**1**) and subsequent alkylation with an appropriate alkyl halide. The 2-alkylpyridines **2-8** were then treated with ethyl bromide to afford the corresponding dialkylpyridinium bromides **9-15**. Optimization of the reaction conditions (concentrations, temperature, reaction time and base) for both metalation and alkylation were described in a previous report.[58] Finally, the subsequent metathesis with bis(trifluoromethane) sulfonimide lithium salt provided the 1-ethyl-2-alkylpyridinium bis(trifluoromethane)sulfonimides **16-22** with excellent purity and overall yield. Their structures were confirmed by ^{1}H NMR, ^{13}C NMR and ESI-HRMS.

Vapor pressure measurements: The vapor pressures of the synthesized ionic liquids were measured at different temperatures using a Knudsen effusion apparatus combined with a quartz crystal microbalance.[55] The experimental vapor pressure data for each ionic liquid is presented in table S1, as supporting information SI. Figure 1 presents the graphical representation of $\ln(p/\mathrm{Pa}) = f\,[(1/T)\,/\,\mathrm{K}^{-1}]$ for the studied ionic liquids. Based on the previous results, the thermodynamic properties of vaporization at the mean temperature, $\langle T \rangle$, and references temperatures, θ, 460 K and 298.15 K, were derived from the fitting of the experimental results of the vapor pressures by the truncated form of the Clarke and Glew equation:[65]

$$R\cdot\ln\frac{p}{p^{\circ}} = -\frac{\Delta_{\mathrm{l}}^{\mathrm{g}}G_{\mathrm{m}}^{\circ}(\theta)}{\theta} + \Delta_{\mathrm{l}}^{\mathrm{g}}H_{\mathrm{m}}^{\circ}(\theta)\cdot\left(\frac{1}{\theta}-\frac{1}{T}\right) + \Delta_{\mathrm{l}}^{\mathrm{g}}C_{p,\mathrm{m}}^{\circ}\cdot\left[\frac{\theta}{T}-1+\ln\left(\frac{T}{\theta}\right)\right] \qquad (1)$$

where p is the vapor pressure, p° is a selected reference pressure ($p^{\circ} = 10^{5}$ Pa), θ is a selected reference temperature, R is the gas constant (R = 8.3144621 J·K^{-1}·mol^{-1})[66] , $\Delta_{\mathrm{l}}^{\mathrm{g}}G_{\mathrm{m}}^{\circ}$ is the standard molar Gibbs energy of vaporization at the selected reference pressure, $\Delta_{\mathrm{l}}^{\mathrm{g}}H_{\mathrm{m}}^{\circ}$ is the standard molar enthalpy of vaporization, and $\Delta_{\mathrm{l}}^{\mathrm{g}}C_{p,\mathrm{m}}^{\circ}$ is the difference between the heat capacities of the gaseous and of the liquid phases [$\Delta_{\mathrm{l}}^{\mathrm{g}}C_{p,\mathrm{m}}^{\circ} = C_{p,\mathrm{m}}^{\circ}(\mathrm{g}) - C_{p,\mathrm{m}}^{\circ}(\mathrm{l})$]. In this work, $\Delta_{\mathrm{l}}^{\mathrm{g}}C_{p,\mathrm{m}}^{\circ}$ = − 100 ± 10 J·K^{-1}·mol^{-1} was considered in the calculations for all ILs under study. The value of (− 100 J·K^{-1}·mol^{-1}) for $\Delta_{\mathrm{l}}^{\mathrm{g}}C_{p,\mathrm{m}}^{\circ}$ is a typical value for liquids and have been used before in the literature[19,52,67] Until recently, temperature correction of the literature values for enthalpies of vaporization have been done using two values of , (−100 J·K^{-1}·mol^{-1}) [30,68–71] and (−40 J·K^{-1}·mol^{-1}) [72,73]. In our previous works [49,50,74], the values of $\Delta_{\mathrm{l}}^{\mathrm{g}}C_{p,\mathrm{m}}^{\circ}$ were estimated for the same temperature, T = 388 K, based on the linear correlation of the literature values [75–78] as a function of the cation's alkyl chain length, using the previously described methodology. [49,50,74] In order to keep consistency with our previous works [49,50,74], in this study we use the same methodology. A recent Monte Carlo simulation study by Rane *et al.* [81] provided additional support for our correlation concerning the $\Delta_{\mathrm{l}}^{\mathrm{g}}C_{p,\mathrm{m}}^{\circ}$ .Table 1 lists the thermodynamic properties of vaporization derived from equation (1) at the mean temperature, $\langle T \rangle$, and references temperatures, θ, 460 K and 298.15 K.

In order to acquire more insights on the effect of the topology of the cation (scheme 2) on the ionic liquid properties, the analysis and rationalization of the obtained thermodynamic properties of vaporization for the [^{2}C$_{N-2}$^{1}C$_{2}$Py][NTf$_{2}$] ionic liquids was done considering the literature data for the [C$_{N-1}$C$_{1}$im][NTf$_{2}$][49,74] and [C$_{N}$Py][NTf$_{2}$] series.[53] The structure of 2-alkyl-1-ethylpyridinium, N-alkylpyridinium and 1-methyl-3-alkylimidazolium cations are presented in scheme 2.

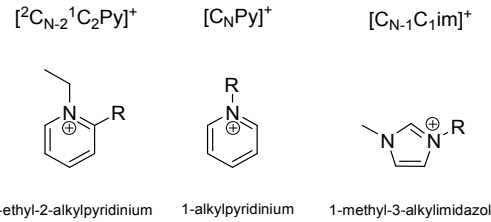

Scheme 2. Structure of 2-alkyl-1-ethylpyridinium, N-alkylpyridinium and 1-methyl-3-alkylimidazolium cations.

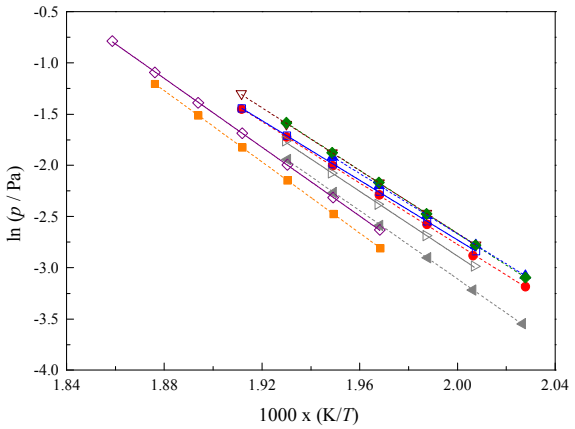

Figure 1. Plot of ln(p/Pa) = f [(1/T) / K^{-1}] for the studied ionic liquid: ● - [^{2}C$_2$^{1}C$_2$Py][NTf$_2$]; □ - [^{2}C$_3$^{1}C$_2$Py][NTf$_2$]; ▲ - [^{2}C$_4$^{1}C$_2$Py][NTf$_2$]; ▽ - [^{2}C$_5$^{1}C$_2$Py][NTf$_2$]; ◆ - [^{2}C$_6$^{1}C$_2$Py][NTf$_2$]; ▷ - [^{2}C$_7$^{1}C$_2$Py][NTf$_2$]; ◀ - [^{2}C$_8$^{1}C$_2$Py][NTf$_2$]; ◇ - [^{2}C$_9$^{1}C$_2$Py][NTf$_2$]; ■ - [^{2}C$_{10}$^{1}C$_2$Py][NTf$_2$].

Table 1. Thermodynamic properties of vaporization derived from the vapor pressure results and the derived standard (p^o = 10^5 Pa), at the reference temperature, θ.

T interval / K	θ / K	$\Delta_l^g G_m^o(\theta)$ / J·mol^{-1}	$\Delta_l^g H_m^o(\theta)$ / J·mol^{-1}	$\Delta_l^g S_m^o(\theta)$ / J·K^{-1}·mol^{-1}	r^2
		[^{2}C$_2$^{1}C$_2$Py][NTf$_2$]			
493 to 524	508.11	58315 ± 978	124553 ± 693	130.4 ± 1.4	0.9998
	460.00	64822 ± 1146	129364 ± 843	140.3 ± 1.7	
	298.15	90787 ± 2753	145549 ± 2211	183.7 ± 5.5	
		[^{2}C$_3$^{1}C$_2$Py][NTf$_2$]			
498 to 524	510.59	57885 ± 617	120929 ± 436	123.5 ± 0.9	0.9999
	460.00	64390 ± 912	125988 ± 668	133.9 ± 1.3	
	298.15	89320 ± 2709	142173 ± 2169	177.3 ± 5.4	
		[^{2}C$_4$^{1}C$_2$Py][NTf$_2$]			
493 to 523	503.12	58554 ± 235	122261 ± 166	126.6 ± 0.3	0.9999
	460.00	64204 ± 636	126573 ± 461	135.6 ± 1.0	
	298.15	89405 ± 2583	142758 ± 2056	178.9 ± 5.2	
		[^{2}C$_5$^{1}C$_2$Py][NTf$_2$]			
498 to 524	510.63	57469 ± 909	127335 ± 643	138.4 ± 1.3	0.9999
	460.00	64656 ± 1111	132398 ± 818	148.9 ± 1.6	
	298.15	91747 ± 2764	148583 ± 2220	192.2 ± 5.5	
		[^{2}C$_6$^{1}C$_2$Py][NTf$_2$]			
493 to 519	505.65	58155 ± 333	128235 ± 235	138.6 ± 0.5	0.9999
	460.00	64694 ± 706	132800 ± 514	148.1 ± 1.1	
	298.15	91913 ± 2619	148985 ± 2088	191.4 ± 5.3	
		[^{2}C$_7$^{1}C$_2$Py][NTf$_2$]			
498 to 519	508.27	58669 ± 1778	131425 ± 1257	143.1 ± 2.5	0.9997
	460.00	65816 ± 1821	136252 ± 1346	153.1 ± 2.7	
	298.15	93855 ± 3011	152437 ± 2448	196.5 ± 5.9	
		[^{2}C$_8$^{1}C$_2$Py][NTf$_2$]			
493 to 519	505.73	59888 ± 1008	138476 ± 712	155.4 ± 1.4	0.9999
	460.00	67208 ± 1152	143049 ± 846	164.9 ± 1.7	
	298.15	97149 ± 2734	159234 ± 2195	208.2 ± 5.5	
		[^{2}C$_9$^{1}C$_2$Py][NTf$_2$]			
508 to 538	523.03	57395 ± 739	139659 ± 531	157.3 ± 1.0	0.9999
	460.00	67705 ± 1073	145962 ± 791	170.1 ± 1.6	
	298.15	98496 ± 2837	162147 ± 2281	213.5 ± 5.7	
		[^{2}C$_{10}$^{1}C$_2$Py][NTf$_2$]			
508 to 560	520.50	58420 ± 898	144487 ± 635	165.4 ± 1.2	0.9999
	460.00	68790 ± 1186	150537 ± 877	177.7 ± 1.7	
	298.15	100809 ± 2870	166722 ± 2312	221.1 ± 5.7	

r^2 is the linear regression coefficient.

Analysing the ln(p/Pa)=f[(1/T)/K^{-1}] representation and considering the experimental temperature range (figure 1), the order of volatility for the [^{2}C$_{N-2}$^{1}C$_2$Py][NTf$_2$] ionic liquids was found to be:

[^{2}C$_4$^{1}C$_2$Py][NTf$_2$] ≈ [^{2}C$_5$^{1}C$_2$Py][NTf$_2$] ≈ [^{2}C$_6$^{1}C$_2$Py][NTf$_2$] > [^{2}C$_2$^{1}C$_2$Py][NTf$_2$] ≈ [^{2}C$_3$^{1}C$_2$Py][NTf$_2$] > [^{2}C$_7$^{1}C$_2$Py][NTf$_2$] > [^{2}C$_8$^{1}C$_2$Py][NTf$_2$] > [^{2}C$_9$^{1}C$_2$Py][NTf$_2$] > [^{2}C$_{10}$^{1}C$_2$Py][NTf$_2$]

The ILs with shorter alkyl chains, [^{2}C$_2$^{1}C$_2$Py][NTf$_2$] and [^{2}C$_3$^{1}C$_2$Py][NTf$_2$], present an outlier behaviour, with lower volatilities than [^{2}C$_4$^{1}C$_2$Py][NTf$_2$], [^{2}C$_5$^{1}C$_2$Py][NTf$_2$] and [^{2}C$_6$^{1}C$_2$Py][NTf$_2$]. The outlier behaviour is similar to the one recently observed in the imidazolium based ILs with short alkyl chain lengths (e.g. [C$_{N-1}$C$_1$im][NTf$_2$] and [C$_{N/2}$C$_{N/2}$im][NTf$_2$]) and arises from the stronger initial effect of the steric hindrance of the alkyl chain on the cation-anion interaction.[49,74]

The graphic representation of the standard molar Gibbs energies of vaporization at reference temperature, T = 460 K, as a function of the total number of carbon atoms in the two alkyl side chains of the cation, N, is presented in figure 2. At the reference temperature, T = 460 K, the 2-alkyl-1-ethylpyridinium based ionic liquids presents significant lower volatility than the imidazolium ionic liquids series.[50]

Analogous to imidazolium based ionic liquids,[49,74] the $\Delta_l^g G_m^o$ profile along the alkyl side chain presents a non-linear behaviour for the ionic liquids with shorter alkyl chain length, with an initial increase of volatility due to the marked steric hindrance of the alkyl chains, reaching a maximum volatility plateau at [^{2}C$_3$^{1}C$_2$Py][NTf$_2$] and [^{2}C$_4$^{1}C$_2$Py][NTf$_2$]. Starting from [^{2}C$_4$^{1}C$_2$Py][NTf$_2$], the volatility decreases along the alkyl side chain length of the cation, similarly as it was observed for the imidazolium series.[50] The non-electrostatic potential is expected to increase nearly linear along the alkyl chain length.[80–82]

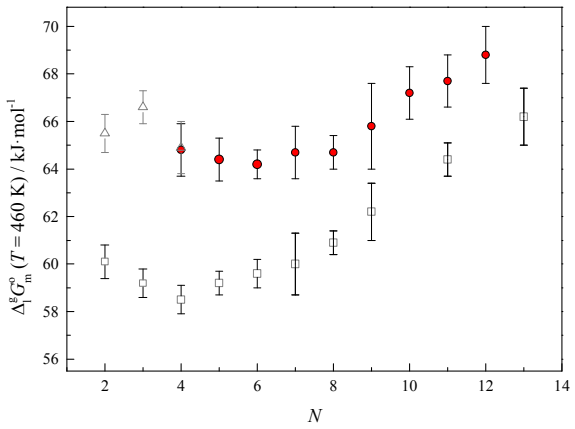

Figure 2. Standard (p^o=10^5 Pa) molar Gibbs energy of vaporization, at T = 460 K, as a function of the total number of carbons in the alkyl side chains of the cation, N. □ - [C$_{N-1}$C$_1$im][NTf$_2$][49,74] (N = 2 - 9, 11, 13); △ - [C$_N$Py][NTf$_2$][53] (N = 2 - 4); ● - [^{2}C$_{N-2}$^{1}C$_2$Py][NTf$_2$] (N = 4 - 12).

The graphic representations of the standard molar enthalpies and entropies of vaporization at reference temperature, T = 460 K, as a function of the total number of carbon atoms in the two alkyl side chains of the cation, N, are presented in figures 3 and 4. The 2-alkyl-1-ethylpyridinium and 1-alkylpyridinium ionic liquids with the shortest alkyl chains, present a significant higher $\Delta_l^g H_m^o$ than the imidazolium series.[50,53] After [^{2}C$_3$^{1}C$_2$Py][NTf$_2$], the difference between the enthalpies of vaporization of the 2-alkyl-1-ethylpyridinium and imidazolium[50,76] ionic liquid families decreases, behing however in all the cases higher indicating that the electrostatic interactions contribution should be slightly higher in the pyridinium based than in the imidazolium ILs .

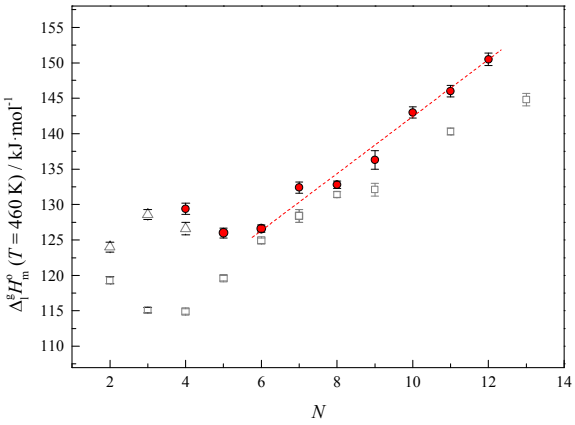

Figure 3. Standard (p^o=10^5 Pa) molar enthalpies of vaporization, at T = 460 K, as a function of the total number of carbons in the alkyl side chains of the cation, N. □ - [$C_{N-1}C_1$im][NTf$_2$][49,74] (N = 2 - 9, 11, 13); △ - [C_NPy][NTf$_2$][53] (N = 2 - 4); ● - [$^2C_{N-2}{}^1C_2$Py][NTf$_2$] (N = 4 - 12).

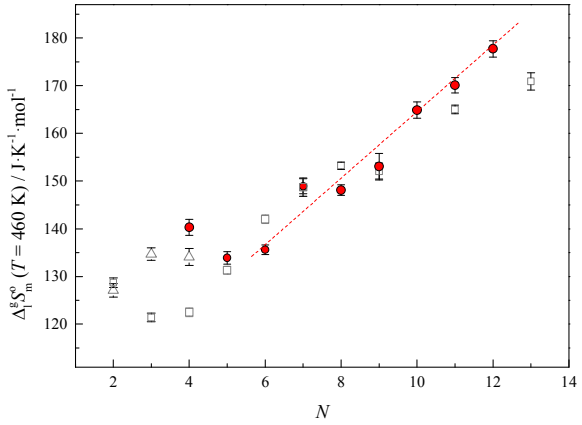

Figure 4. Standard (p^o=10^5 Pa) molar entropies of vaporization, at T = 460 K, as a function of the total number of carbons in the alkyl side chains of the cation, N. □ - [$C_{N-1}C_1$im][NTf$_2$][49,74] (N = 2 - 9, 11, 13); △ - [C_NPy][NTf$_2$][53] (N = 2 - 4); ● - [$^2C_{N-2}{}^1C_2$Py][NTf$_2$] (N = 4 - 12).

The overview of the entropies of vaporization along the series (figure 4) shows a similar profile than the one of $\Delta_l^g H_m^o$, however the differentiation between the ionic liquid families, focused in this work, is smaller for $\Delta_l^g S_m^o$.[49,52,74] A decrease of the entropy from [$^2C_2{}^1C_2$Py][NTf$_2$] to [$^2C_3{}^1C_2$Py][NTf$_2$] is observed, and is related with an increase of the alkyl chain contribution to the entropy of the liquid. After [$^2C_3{}^1C_2$Py][NTf$_2$], the entropies of vaporization increases along the series and follows the same trend than the observed in the imidazolium based ionic liquids series.[49,74] It is interesting to observed that due to the enthalpic-entropic compensation effect the [$^2C_2{}^1C_2$Py][NTf$_2$] and [C_4Py][NTf$_2$][53] present similar volatilities in where the [$^2C_2{}^1C_2$Py][NTf$_2$] presents higher enthalpies and entropies of vaporization than the isomer [C_4Py][NTf$_2$].[53] From the analysis of the enthalpic and entropic contribution to the volatility of the ionic liquids under study, it was found that the lower volatility of the [$^2C_{N-2}{}^1C_2$Py][NTf$_2$] ionic liquids, when compared with the [$C_{N-1}C_1$im][NTf$_2$] series, is mainly due to the higher enthalpies of vaporization.

Electrospray ionization mass spectrometry (ESI-MS-MS): Electrospray ionization mass spectrometry data were further used to gather additional insights into the interpretation of the thermodynamic properties of vaporization in terms of the IL's interaction energies. The mass spectral data, represented as $E_{cm,1/2}$, for the novel pyridinium based ionic liquids, [$^2C_{N-2}{}^1C_2$Py][NTf$_2$], as well as, for the 1-alkylpyridinium based ionic liquids, [C_NPy][NTf$_2$] (N=2 – 9), as listed in table 2 and plotted as a function of the total number of carbon atoms in the alkyl side chains, as well as, the longer alkyl size of the pyridinium cation figure 5. In both series of ILs the variation of the relative cation-anion interactions, expressed by the experimental energies $E_{lab,1/2}$ and the calculated dissociation energies $E_{cm,1/2}$ values, for the following reaction:

$$[(\text{cation})^2(\text{anion})]^+ + \rightarrow [(\text{cation})(\text{anion})] + (\text{cation})^+$$

Using the procedure and methodology described previously in the literature.[53] The ESI-MS-MS data show a very identical trend with the increase of the cation side alkyl chain length for both series if the total number of carbons in the alkyl chain is consider. A pronounced initial decrease of the relative cation-anion (ion pair) interaction energy reaching an almost constant value for $E_{cm,1/2}$, reflecting the increase of the alkyl group hindrance in the cation to ion pair interaction until C_6.

Table 2. $E_{lab,1/2}$ and $E_{cm,1/2}$, for the novel pyridinium based ionic liquids, [$^2C_{N-2}{}^1C_2$Py][NTf$_2$], (N = 4 - 12).

Ionic liquid	[(cation)$_2$anion]$^+$	
	$E_{lab,1/2}$ /eV	$E_{cm,1/2}$ / eV
[$^2C_2{}^1C_2$Py][NTf$_2$]	9.4	0.64
[$^2C_3{}^1C_2$Py][NTf$_2$]	7.7	0.50
[$^2C_4{}^1C_2$Py][NTf$_2$]	7.0	0.43
[$^2C_5{}^1C_2$Py][NTf$_2$]	6.9	0.41
[$^2C_6{}^1C_2$Py][NTf$_2$]	7.2	0.41
[$^2C_7{}^1C_2$Py][NTf$_2$]	7.7	0.42
[$^2C_8{}^1C_2$Py][NTf$_2$]	7.8	0.41
[$^2C_9{}^1C_2$Py][NTf$_2$]	8.4	0.43
[$^2C_{10}{}^1C_2$Py][NTf$_2$]	8.7	0.43
[C_2Py][NTf$_2$]	12.7	0.95
[C_3Py][NTf$_2$]	10.8	0.77
[C_4Py][NTf$_2$]	9.5	0.64 (0.50) [a]
[C_5Py][NTf$_2$]	7.9	0.51
[C_6Py][NTf$_2$]	7.5	0.46 (0.45) [a]
[C_7Py][NTf$_2$]	7.6	0.45
[C_8Py][NTf$_2$]	7.9	0.45 (0.45) [a]
[C_9Py][NTf$_2$]	7.9	0.43

Average Standard deviation of $E_{cm,1/2}$ ± 0.01 eV. [(a)] Reference [62].

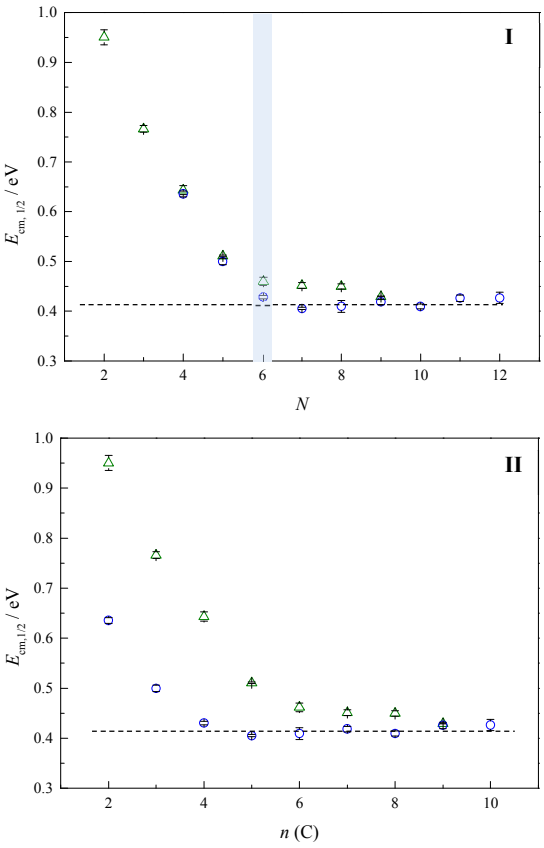

Figure 5. $E_{cm,1/2}$ dependency with the total number of carbon atoms in the alkyl side chains, *N*, (**I**) and with the longer alkyl size chain, *n*(C), (**II**) of the pyridinium cation. △ - $[C_NPy][NTf_2]$ (N = *n*(C) = 2 - 4); ○ - $[^2C_{N-2}{}^1C_2Py][NTf_2]$ (N = 4 – 12; *n*(C) = N-2)

Conclusions:

This work is a contribution to the molecular understanding of the thermodynamics and cohesive energy of pyridinium based ionic liquids and presents the detailed synthesis, characterization and volatility study of new pyridinium based ionic liquids, $[^2C_{N-2}{}^1C_2Py][NTf_2]$ (N= 2 − 12) which show higher thermal stability and lower volatility than the imidazolium based ionic liquids.

The shape of the relative cation-anion (ion pair) interaction derived from ESI-MS-MS is in agreement with the shape and interpretation derived from the Gibbs energy of vaporization. The initial increase of volatility is due to the decrease of the enthalpies of vaporization indicating that the change of direct cation to (ion pair) interactions is reflected as expected in the magnitude of the IL cohesive energy.

The volatility trend reflects the overlapping of the two main interaction potentials in the liquid: electrostatic and non-electrostatic, reaching a nearly linear increment of the Gibbs energy of vaporization (volatility decrease) after $[C_3C_1im][NTf_2]$[50] and $[^2C_3{}^1C_2Py][NTf_2]$. As observed in the cation-anion (ion pair) interaction, the electrostatic potential decreases initially until a stationary value at C_6 that is overlapped by the nearly linear van der Waals interaction functional (non-electrostatic interaction potential) as is presented scheme 3.

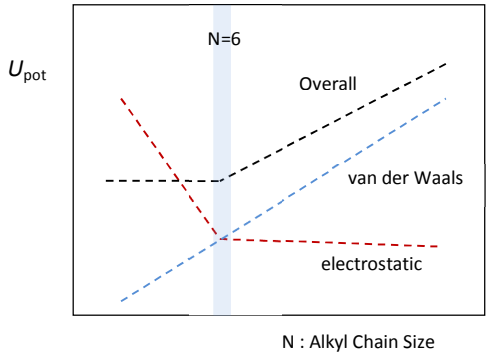

Scheme 3. Schematic diagram of the interaction potential, U_{pot} change with the alkyl chain size, *N*.

Experimental Section

Materials

Chemicals used in the synthesis: 2-Picoline (Acros organics, 98%), *n*-butyllithium (Sigma–Aldrich, 2.5 M in hexane), iodomethane (Acros organics, 99%, stabilized), bromoethane (Acros organics, 98%), 1-bromopropane (Acros organics, 99%), 1-bromobutane (Sigma–Aldrich, 99%), 1-iodopentane (Sigma–Aldrich, 98%, stabilized), 1-iodohexane (Sigma–Aldrich, 98%, stabilized), 1-bromoheptane (Acros organics, 99%), 1-bromooctane (Acros organics, 99%), 1-bromononane (Acros organics, 97%), bis(trifluoromethanesulfonyl)imide lithium salt (Sigma-Aldrich, 99%) and acetonitrile (Sigma–Aldrich, ACS reagent, ≥99.5%) were commercially available and used without any further pre-treatment or pre-purification, except tetrahydrofuran (Panreac, 99.5%, stabilized),which was dried with suitable drying agents and distilled under argon prior to use.

General Methods: ^1H and ^{13}C NMR spectra of the obtained products were recorded in $CDCl_3$ on a Bruker ARX at 400.1621 and 100.6314 MHz respectively. Chemical shifts are reported in parts per million (ppm, δ) and coupling constants (*J*) in hertz. ESI mass spectra were recorded on an apex-Qe spectrometer.

General procedure for 2-picoline alkylation: A solution of 2-picoline (5 mL, 49.5 mmol) in anhydrous THF (75 mL) was introduced into a 250 mL round flask under inert atmosphere. The mixture was cooled to -78 °C with a dry ice-acetone bath and a solution of *n*-BuLi 2.5 M in hexane (19.8 mL, 49.5 mmol) was then slowly added over 10 min. After stirring for 1h, while keeping the temperature below -20 °C, the obtained deep red solution was cooled again to -78 °C and a solution of the appropriate 1-alkyl halide (2 equiv.) in anhydrous THF (50 mL) was slowly added. The reaction mixture was allowed to gradually warm up to room temperature and stirred for 1 to 5 h depending on the 1-alkyl halide. The reaction progress was monitored by t.l.c using silica gel 60 GF-254 aluminium sheets and hexane/ethyl acetate (1/1) as eluent. The reaction was worked up by adding of water (25 mL), neutralized with a saturated solution of ammonium chloride (25 mL) and extracted with dichloromethane (3 x 25 mL). The organic extracts were combined, dried over Na_2SO_4 and filtered. The solvent was removed on the rotary evaporator and the residue was further purified by chromatography over silica gel using gradient elution (starting with hexane to hexane/ethyl acetate 1.5/1). All synthesized 2-alkylpyridines were obtained as slightly yellow liquids.

2-Ethylpyridine (2).[83] Yield 83%. ^{1}H NMR (400 MHz, [D$_1$]CDCl$_3$, 25°C, TMS): δ=8.49 (ddd, *J*(H,H)=0.8 Hz, *J*(H,H)=1.7 Hz, *J*(H,H)=4.8 Hz, 1H; H-6), 7.56 (td, *J*(H,H)=1.9 Hz, *J*(H,H)=7.7 Hz, 1H; H-4), 7.12 (d, *J*(H,H)=7.8 Hz, 1H; H-3), 7.06 (m, 1H; H-5), 2.79 (q, *J*(H,H)=7.6 Hz, 2H; 1´-Et), 1.28 (t, *J*(H,H)=7.6 Hz, 3H; 2´-Et). ^{13}C NMR (100 MHz, [D$_1$]CDCl$_3$, 25°C, TMS): δ=162.9 (C-2), 148.6 (C-6), 135.8 (C-4), 121.5 (C-3), 120.4 (C-5), 30.9 (1´-Et), 13.4 (2´-Et).

2-Propylpyridine (3).[84] Yield 87%. ^{1}H NMR (400 MHz, [D$_1$]CDCl$_3$, 25°C, TMS): δ= 8.48 (ddd, *J*(H,H)=0.8 Hz, *J*(H,H)=1.7 Hz, *J*(H,H)=4.8 Hz, 1H; H-6), 7.53 (td, *J*(H,H)=1.6 Hz, *J*(H,H)=7.7 Hz, 1H; H-4), 7.09 (d, *J*(H,H)=7.8 Hz, 1H; H-3), 7.04 (m, 1H; H-5), 2.72 (m, 2H; 1´-Pr), 1.72 (m, 2H; 2´-Pr), 0.93 (t, *J*(H,H)=7.4 Hz, 3H; 3´-Pr). ^{13}C NMR (100 MHz, [D$_1$]CDCl$_3$, 25°C, TMS): δ=162.1 (C-2), 149.1 (C-6), 136.0 (C-4), 122.6 (C-3), 120.7 (C-5), 40.3 (1´-Pr), 23.0 (2´-Pr), 13.7 (3´-Pr).

2-Butylpyridine (4).[85] Yield 82%. ^{1}H NMR (400 MHz, [D$_1$]CDCl$_3$, 25°C, TMS): δ=8.49 (ddd, *J*(H,H)=0.8 Hz, *J*(H,H)=1.7 Hz, *J*(H,H)=4.9 Hz, 1H; H-6), 7.54 (td, *J*(H,H)=1.9 Hz, *J*(H,H)=7.7 Hz, 1H; H-4), 7.10 (d, *J*(H,H)=7.8 Hz, 1H; H-3), 7.05 (ddd, *J*(H,H)=1.0 Hz, *J*(H,H)=4.9 Hz, *J*(H,H)=7.5 Hz, 1H; H-5), 2.75 (m, 2H; 1´-Bu), 1.68 (m, 2H; 2´-Bu), 1.35 (m, 2H; 3´-Bu), 0.91 (t, *J*(H,H)=7.4 Hz, 3H; 4´-Bu). ^{13}C NMR (100 MHz, [D$_1$]CDCl$_3$, 25°C, TMS): δ=162.4 (C-2), 149.1 (C-6), 136.1 (C-4), 122.6 (C-3), 120.7 (C-5), 38.1 (1´-Bu), 32.0 (2´-Bu), 22.4 (3´-Bu), 13.9 (4´-Bu).

2-Pentylpyridine (5).[86] Yield 85%. ^{1}H NMR (400 MHz, [D$_1$]CDCl$_3$, 25°C, TMS): δ=8.48 (ddd, *J*(H,H)=0.8 Hz, *J*(H,H)=1.7 Hz, *J*(H,H)=4.9 Hz, 1H; H-6), 7.53 (td, *J*(H,H)=1.9 Hz, *J*(H,H)=7.7 Hz, 1H; H-4), 7.09 (d, *J*(H,H)=7.8 Hz, 1H; H-3), 7.04 (ddd, *J*(H,H)=1.0 Hz, *J*(H,H)=4.9 Hz, *J*(H,H)=7.4 Hz, 1H; H-5), 2.74 (m, 2H; 1´-Pen), 1.69 (m, 2H; 2´-Pen), 1.30 (m, 4H; 3´,4´-Pen), 0.85 (t, *J*(H,H)=7.0 Hz, 3H; 5´-Pen). ^{13}C NMR (100 MHz, [D$_1$]CDCl$_3$, 25°C, TMS): δ=162.5 (C-2), 149.2 (C-6), 136.2 (C-4), 122.7 (C-3), 120.8 (C-5), 38.4 (1´-Pen), 31.6 (3´-Pen), 29.6 (2´-Pen), 22.5 (4´-Pen), 14.0 (5´-Pen).

2-Hexylpyridine (6).[87] Yield 85%. ^{1}H NMR (400 MHz, [D$_1$]CDCl$_3$, 25°C, TMS): δ=8.51 (ddd, *J*(H,H)=0.8 Hz, *J*(H,H)=1.7 Hz, *J*(H,H)=4.9 Hz, 1H; H-6), 7.56 (td, *J*(H,H)=1.9 Hz, *J*(H,H) = 7.7 Hz, 1H; H-4), 7.12 (d, *J*(H,H)=7.8 Hz, 1H; H-3), 7.07 (ddd, *J*(H,H)=1.0 Hz, *J*(H,H)=4.9 Hz, *J*(H,H)=7.4 Hz, 1H; H-5), 2.76 (m, 2H; 1´-Hex), 1.71 (m, 2H; 2´-Hex), 1.32 (m, 6H; 3´,4´,5´-Hex), 0.86 (t, *J*(H,H)=7.1 Hz, 3H; 6´-Hex). ^{13}C NMR (100 MHz, [D$_1$]CDCl$_3$, 25°C, TMS): δ=162.5 (C-2), 149.2 (C-6), 136.2 (C-4), 122.7 (C-3), 120.8 (C-5), 38.5 (1´-Hex), 31.7 (4´-Hex), 29.9 (2´-Hex), 29.1 (3´-Hex), 22.6 (5´-Hex), 14.1 (6´-Hex).

2-Heptylpyridine (7).[88] Yield 79%. ^{1}H NMR (400 MHz, [D$_1$]CDCl$_3$, 25°C, TMS): δ=8.49 (ddd, *J*(H,H)=0.8 Hz, *J*(H,H)=1.7 Hz, *J*(H,H)=4.9 Hz, 1H; H-6), 7.53 (td, *J*(H,H)=1.9 Hz, *J*(H,H)=7.7 Hz, 1H; H-4), 7.10 (d, *J*(H,H)=7.8 Hz, 1H; H-3), 7.04 (ddd, *J*(H,H)=1.0 Hz, *J*(H,H)=4.9 Hz, *J*(H,H)=7.5 Hz, 1H; H-5), 2.75 (m, 2H; 1´-Hep), 1.70 (m, 2H; 2´-Hep), 1.30 (m, 8H; 3´,4´,5´,6´-Hep), 0.84 (t, *J*(H,H)=6.9 Hz, 3H; 7´-Hep). ^{13}C NMR (100 MHz, [D$_1$]CDCl$_3$, 25°C, TMS): δ=162.4 (C-2), 149.0 (C-6), 136.0 (C-4), 122.5 (C-3), 120.7 (C-5), 38.3 (1´-Hep), 31.6 (5´-Hep), 29.8 (2´-Hep), 29.2* (4´-Hep), 29.0* (3´-Hep), 22.5 (6´-Hep), 14.0 (7´-Hep).

2-Octylpyridine (8).[89] Yield 83%. ^{1}H NMR (400 MHz, [D$_1$]CDCl$_3$, 25°C, TMS): δ=8.49 (ddd, *J*(H,H)=0.8 Hz, *J*(H,H)=1.7 Hz, *J*(H,H)=4.9 Hz, 1H; H-6), 7.54 (td, *J*(H,H)=1.9 Hz, *J*(H,H)=7.7 Hz, 1H; H-4), 7.10 (d, *J*(H,H)=7.8 Hz, 1H; H-3), 7.05 (ddd, *J*(H,H)=1.0 Hz, *J*(H,H)=4.9 Hz, *J*(H,H)=7.5 Hz, 1H; H-5), 2.75 (m, 2H; 1´-Oc), 1.69 (m, 2H; 2´-Oc), 1.28 (m, 10H; 3´,4´,5´,6´,7´-Oc), 0.84 (t, *J*(H,H)=6.9 Hz, 3H; 8´-Oc). ^{13}C NMR (100 MHz, [D$_1$]CDCl$_3$, 25°C, TMS): δ=162.4 (C-2), 149.0 (C-6), 136.1 (C-4), 122.6 (C-3), 120.7 (C-5), 38.4 (1´-Oc), 31.8 (6´-Oc), 29.9 (2´-Oc), 29.4* (4´-Oc), 29.3* (3´-Oc), 29.1* (5´-Oc), 22.6 (7´-Oc), 14.0 (8´-Oc).

2-Nonylpyridine (9). Yield 89%. ^{1}H NMR (400 MHz, [D$_1$]CDCl$_3$, 25°C, TMS): δ=8.47 (ddd, *J*(H,H)=0.8 Hz, *J*(H,H)=1.7 Hz, *J*(H,H)=4.9 Hz, 1H; H-6), 7.52 (td, *J*(H,H)=1.9 Hz, *J*(H,H)=7.7 Hz, 1H; H-4), 7.08 (d, *J*(H,H)=7.8 Hz, 1H; H-3), 7.03 (ddd, *J*(H,H)=1.0 Hz, *J*(H,H)=4.9 Hz, *J*(H,H)=7.4 Hz, 1H; H-5), 2.73 (m, 2H; 1´-Non), 1.68 (m, 2H; 2´-Non), 1.27 (m, 12H; 3´,4´,5´,6´,7´,8´-Non), 0.82 (t, *J*(H,H)=6.9 Hz, 3H; 9´-Non). ^{13}C NMR (100 MHz, [D$_1$]CDCl$_3$, 25°C, TMS): δ=162.8 (C-2), 149.3 (C-6), 136.3 (C-4), 122.7 (C-3), 120.8 (C-5), 38.0 (1´-Non), 31.4 (7´-Non), 29.4* (4´-Non), 29.0* (5´-Non), 29.0* (6´-Non), 28.9* (3´-Non), 28.8* (2´-Non), 22.1 (8´-Non), 13.5 (9´-Non).

2-Decylpyridine (10).[90] Yield 92%. ^{1}H NMR (400 MHz, [D$_1$]CDCl$_3$, 25°C, TMS): δ= 8.49 (ddd, *J*(H,H)=0.8 Hz, *J*(H,H)=1.7 Hz, *J*(H,H)=4.9 Hz, 1H; H-6), 7.51 (td, *J*(H,H)=1.9 Hz, *J*(H,H)=7.7 Hz, 1H; H-4), 7.08 (d, *J*(H,H)=7.8 Hz, 1H; H-3), 7.01 (ddd, *J*(H,H)=1.0 Hz, *J*(H,H)=4.9 Hz, *J*(H,H)=7.4 Hz, 1H; H-5), 2.76 (m, 2H; 1´-Dec), 1.65 (m, 2H; 2´-Dec), 1.32 (m, 14H; 3´,4´,5´,6´,7´,8´,9´-Dec), 0.88 (t, *J*(H,H)=6.9 Hz, 3H; 10´-Dec). ^{13}C NMR (100 MHz, [D$_1$]CDCl$_3$, 25°C, TMS): δ=162.4 (C-2), 149.0 (C-6), 135.9 (C-4), 122.3 (C-3), 120.5 (C-5), 37.6 (1´-Dec), 31.1 (8´-Dec), 29.1* (4´-Dec), 28.8* (5´,6´-Dec), 28.7* (7´-Dec), 28.6* (2´,3´-Dec), 21.9 (9´-Dec), 13.2 (10´-Dec).

General procedures for the synthesis of 1-ethyl-2-alkylpyridinium bromides

Bromoethane (5 equivalents) was added dropwise to a solution of the corresponding 2-alkylpyridine in acetonitrile (5 mL per mmol of starting 2-alkylpyridine). The reaction mixture was stirred at reflux until completion. The reaction progress was monitored by t.l.c using silica gel 60 GF-254 aluminium sheets and CH_2Cl_2/CH_3OH (95/5) as eluent. After removing the solvent under reduced pressure, the residue was purified by Al_2O_3 chromatography (neutral, activity II-III), using gradient elution (starting with CH_2Cl_2 to CH_2Cl_2/CH_3OH 9/1). The resulting fractions were combined and the solvent removed under reduced pressure to give the desired 1-ethyl-2-alkylpyridinium bromide that were dried by heating at 60 °C and stirring under high vacuum (2 x 10^{-1} Pa) for 48 h. All the synthesized 1-ethyl-2-alkylpyridinium bromides were obtained as slightly yellow and very viscous liquids, except the compounds 9 and 10 which were obtained as white solid and semisolid, respectively.

1,2-Diethylpyridinium bromide (11). Yield 96%. ^{1}H NMR (400 MHz, [D$_1$]CDCl$_3$, 25°C, TMS): δ=9.70 (dd, *J*(H,H)=1.1 Hz, *J*(H,H)=6.2 Hz, 1H; H-6), 8.47 (td, *J*(H,H)=1.4 Hz, *J*(H,H)=7.9 Hz, 1H; H-4), 7.94 (m, 2H ; H-3, H-5), 4.93 (q, *J*(H,H)=7.3 Hz, 2H; NC*H*$_2$CH$_3$), 3.21 (q, *J*(H,H)=7.5 Hz, 2H; 1´-Et), 1.60 (t, *J*(H,H)=7.3 Hz, 3H; NCH$_2$C*H*$_3$), 1.42 (t, *J*(H,H)=7.5 Hz, 3H; 2´-Et). ^{13}C NMR (100 MHz, [D$_1$]CDCl$_3$, 25°C, TMS): δ=158.6 (C-2), 146.2 (C-6),

145.4 (C-4), 127.9 (C-3), 126.2 (C-5), 53.1 (NCH_2CH_3), 25.7 (1′-Et), 16.6 (NCH_2CH_3), 12.5 (2′-Et). ESI-HRMS (apex-Qe): m/z (%): 566.17302 (6) $[(C_9H_{14}N)_3\ (Br)_2]^+$ calcd for 566.17400), 352 (9) $[(C_9H_{14}N)_2\ (Br) + 1]^+$, 351.14263 (43) $[(C_9H_{14}N)_2\ (Br)]^+$ calcd for 351.14304), 136 (100) $[(C_9H_{14}N)]^+$.

1-Ethyl-2-propylpyridinium bromide (12). Yield 94%. ^{1}H NMR (400 MHz, $[D_1]CDCl_3$, 25°C, TMS): δ= 9.71 (dd, *J*(H,H)=1.1 Hz, *J*(H,H)=6.2 Hz, 1H; H-6), 8.45 (td, *J*(H,H)=1.5 Hz, *J*(H,H)=7.9 Hz, 1H; H-4), 7.92 (m, 2H; H-3, H-5), 4.89 (q, *J*(H,H)=7.3 Hz, 2H; NCH_2CH_3), 3.08 (m, 2H; 1′-Pr), 1.78 (m, 2H; 2′-Pr), 1.59 (t, *J*(H,H)=7.3 Hz, 3H; NCH_2CH_3), 1.03 (t, *J*(H,H)=7.3 Hz, 3H; 3′-Pr). ^{13}C NMR (100 MHz, $[D_1]CDCl_3$, 25°C, TMS): δ=157.3 (C-2), 146.2 (C-6), 145.2 (C-4), 128.8 (C-3), 126.2 (C-5), 53.0 (NCH_2CH_3), 34.0 (1′-Pr), 21.9 (2′-Pr), 16.7 (NCH_2CH_3), 13.5 (3′-Pr). ESI-HRMS (apex-Qe): m/z (%): 837 (47) $[(C_{10}H_{16}N)_4\ (Br)_3]^+$, 608 (24) $[(C_{10}H_{16}N)_3\ (Br)_2]^+$, 379.17400 (100) $[(C_{10}H_{16}N)_2\ (Br)]^+$ calcd for 379.17434).

2-Butyl-1-ethylpyridinium bromide (13). Yield 95%. ^{1}H NMR (400 MHz, $[D_1]CDCl_3$, 25°C, TMS): δ=9.62 (dd, *J*(H,H)=1.0 Hz, *J*(H,H)=6.2 Hz, 1H; H-6), 8.41 (td, *J*(H,H)=1.5 Hz, *J*(H,H)=7.9 Hz, 1H; H-4), 7.86 (m, 2H; H-3, H-5), 4.82 (q, *J*(H,H)=7.3 Hz, 2H; NCH_2CH_3), 3.03 (m, 2H; 1′-Bu), 1.64 (m, 2H; 2′-Bu), 1.53 (t, *J*(H,H)=7.3 Hz, 3H; NCH_2CH_3), 1.37 (m, 2H; 3′-Bu), 0.84 (t, *J*(H,H)=7.3 Hz, 3H; 4′-Bu). ^{13}C NMR (100 MHz, $[D_1]CDCl_3$, 25°C, TMS): δ=157.3 (C-2), 146.1 (C-6), 145.2 (C-4), 128.6 (C-3), 126.1 (C-5), 52.8 (NCH_2CH_3), 31.8 (1′-Bu), 30.3 (2′-Bu), 22.0 (3′-Bu), 16.6 (NCH_2CH_3), 13.3 (4′-Bu). ESI-HRMS (apex-Qe): m/z (%): 893 (27) $[(C_{11}H_{18}N)_4\ (Br)_3]^+$, 650 (17) $[(C_{11}H_{18}N)_3\ (Br)_2]^+$, 407.20529 (100) $[(C_{11}H_{18}N)_2\ (Br)]^+$ calcd for 407.20564).

1-Ethyl-2-pentylpyridinium bromide (14). Yield 91%. ^{1}H NMR (400 MHz, $[D_1]CDCl_3$, 25°C, TMS): δ=9.69 (dd, *J*(H,H)=1.0 Hz, *J*(H,H)=6.1 Hz, 1H; H-6), 8.43 (td, *J*(H,H)=1.3 Hz, *J*(H,H)=7.9 Hz, 1H; H-4), 7.88 (m, 2H; H-3, H-5), 4.85 (q, *J*(H,H)=7.3 Hz, 2H; NCH_2CH_3), 3.04 (m, 2H; 1′-Pen), 1.68 (m, 2H; 2′-Pen), 1.55 (t, *J*(H,H)=7.3 Hz, 3H; NCH_2CH_3), 1.37-1.20 (m, 4H; 3′,4′-Pen), 0.78 (t, *J*(H,H)=7.2 Hz, 3H; 5′-Pen). ^{13}C NMR (100 MHz, $[D_1]CDCl_3$, 25°C, TMS): δ=157.4 (C-2), 146.1 (C-6), 145.2 (C-4), 128.7 (C-3), 126.1 (C-5), 52.8 (NCH_2CH_3), 32.1 (1′-Pen), 30.9 (3′-Pen), 28.1 (2′-Pen), 21.9 (4′-Pen), 16.6 (NCH_2CH_3), 13.5 (5′-Pen). ESI-HRMS (apex-Qe): m/z (%): 949 (23) $[(C_{12}H_{20}N)_4\ (Br)_3]^+$, 692 (25) $[(C_{12}H_{20}N)_3\ (Br)_2]^+$, 435.23641 (100) $[(C_{12}H_{20}N)_2\ (Br)]^+$ calcd for 435.23694).

1-Ethyl-2-hexylpyridinium bromide (15). Yield 97%. ^{1}H NMR (400 MHz, $[D_1]CDCl_3$, 25°C, TMS): δ=9.58 (dd, *J*(H,H)=1.1 Hz, *J(H,H)*=6.3 Hz, 1H; H-6), 8.38 (td, *J*(H,H)=1.4 Hz, *J*(H,H)=7.9 Hz, 1H; H-4), 7.84 (dd, *J*(H,H)=1.1 Hz, *J*(H,H)=8.1 Hz, 1H; H-3), 7.79 (m, 1H; H-5), 4.76 (q, *J*(H,H)=7.3 Hz, 2H; NCH_2CH_3), 2.97 (m, 2H; 1′-Hex), 1.59 (m, 2H; 2′-Hex), 1.47 (t, *J*(H,H)=7.3 Hz, 3H; NCH_2CH_3), 1.27 (m, 2H; 3′-Hex), 1.10 (m, 4H; 4′,5′-Hex), 0.66 (t, *J*(H,H)=7.1 Hz, 3H; 6′-Hex). ^{13}C NMR (100 MHz, $[D_1]CDCl_3$, 25°C, TMS): δ=157.2 (C-2), 145.8 (C-6), 145.1 (C-4), 128.6 (C-3), 125.9 (C-5), 52.6 (NCH_2CH_3), 31.9 (1′-Hex), 30.7 (4′-Hex), 28.3 (2′-Hex), 28.2 (3′-Hex), 21.8 (5′-Hex), 16.4 (NCH_2CH_3), 13.4 (6′-Hex). ESI-HRMS (apex-Qe): m/z (%): 1005 (21) $[(C_{13}H_{22}N)_4\ (Br)_3]^+$, 734 (39) $[(C_{13}H_{22}N)_3\ (Br)_2]^+$, 463.26771 (100) $[(C_{13}H_{22}N)_2\ (Br)]^+$ calcd for 463.26824).

1-Ethyl-2-heptylpyridinium bromide (16). Yield 94%. ^{1}H NMR (400 MHz, $[D_1]CDCl_3$, 25°C, TMS): δ=9.65 (dd, *J*(H,H)=1.1 Hz, *J*(H,H)=6.3 Hz, 1H; H-6), 8.41 (td, *J*(H,H)=1.4 Hz, *J*(H,H)=7.9 Hz, 1H; H-4), 7.84 (m, 2H; H-3, H-5), 4.81 (q, *J*(H,H)=7.3 Hz, 2H; NCH_2CH_3), 3.01 (m, 2H; 1′-Hep), 1.63 (m, 2H; 2′-Hep), 1.51 (t, *J*(H,H)=7.3 Hz, 3H; NCH_2CH_3), 1.30 (m, 2H; 3′-Hep), 1.21-1.04 (m, 6H; 4′,5′,6′-Hep), 0.69 (t, *J*(H,H)=6.9 Hz, 3H; 7′-Hep). ^{13}C NMR (100 MHz, $[D_1]CDCl_3$, 25°C, TMS): δ=157.3 (C-2), 146.0 (C-6), 145.2 (C-4), 128.6 (C-3), 126.0 (C-5), 52.7 (NCH_2CH_3), 32.1 (1′-Hep), 31.0 (5′-Hep), 28.7* (2′-Hep), 28.4* (4′-Hep), 28.3* (3′-Hep), 22.0 (6′-Hep), 16.5 (NCH_2CH_3), 13.6 (7′-Hep). ESI-HRMS (apex-Qe): m/z (%): 1061 (4) $[(C_{14}H_{24}N)_4\ (Br)_3]^+$, 776 (10) $[(C_{14}H_{24}N)_3\ (Br)_2]^+$, 491.29923 (64) $[(C_{14}H_{24}N)_2\ (Br)]^+$ calcd for 491.29954), 206.19024 (100) $[(C_{14}H_{24}N)]^+$ calcd for 206.19033).

1-Ethyl-2-octylpyridinium bromide (17). Yield 96%. ^{1}H NMR (400 MHz, $[D_1]CDCl_3$, 25°C, TMS): δ=9.81 (dd, *J*(H,H)=1.1 Hz, *J*(H,H)=6.3 Hz, 1H; H-6), 8.45 (td, *J*(H,H)=1.0 Hz, *J*(H,H)=7.9 Hz, 1H; H-4), 7.96 (m, 1H; H-3), 7.88 (m, 1H; H-5), 4.94 (q, *J*(H,H)=7.3 Hz, 2H; NCH_2CH_3), 3.09 (m, 2H; 1′-Oc), 1.75 (m, 2H; 2′-Oc), 1.63 (t, *J*(H,H)=7.3 Hz, 3H; NCH_2CH_3), 1.42 (m, 2H; 3′-Oc), 1.35-1.13 (m, 8H; 4′,5′,6′,7′-Oc), 0.82 (t, *J*(H,H)=6.9 Hz, 3H; 8′-Oc). ^{13}C NMR (100 MHz, $[D_1]CDCl_3$, 25°C, TMS): δ=157.1 (C-2), 145.8 (C-6), 145.1 (C-4), 128.5 (C-3), 125.9 (C-5), 52.6 (NCH_2CH_3), 31.9 (1′-Oc), 31.1 (6′-Oc), 28.6* (2′-Oc), 28.6* (4′-Oc), 28.4* (3′-Oc), 28.2* (5′-Oc), 22.0 (7′-Oc), 16.4 (NCH_2CH_3), 13.5 (8′-Oc). ESI-HRMS (apex-Qe): m/z (%): 1118 (10) $[(C_{15}H_{26}N)_4\ (Br)_3]^+$, 818 (11) $[(C_{15}H_{26}N)_3\ (Br)_2]^+$, 519.33005 (100) $[(C_{15}H_{26}N)_2\ (Br)]^+$ calcd for 519.33084), 220.20583 (79) $[(C_{15}H_{26}N)]^+$ calcd for 220.20598).

1-Ethyl-2-nonylpyridinium bromide (18). Yield 95%. ^{1}H NMR (400 MHz, $[D_1]CDCl_3$, 25°C, TMS): δ=9.81 (dd, *J*(H,H)=1.2 Hz, *J*(H,H)=6.3 Hz, 1H; H-6), 8.46 (td, *J*(H,H)=1.4 Hz, *J*(H,H)=7.9 Hz, 1H; H-4), 7.98 (m, 1H; H-3), 7.88 (m, 1H; H-5), 4.94 (q, *J*(H,H)=7.3 Hz, 2H; NCH_2CH_3), 3.10 (m, 2H; 1′-Non), 1.84 (m, 2H; 2′-Non), 1.70 (t, *J*(H,H)=7.3 Hz, 3H; NCH_2CH_3), 1.45 (m, 2H; 3′-Non), 1.33-1.13 (m, 10H; 4′,5′,6′,7′,8′-Non), 0.83 (t, *J*(H,H)=6.9 Hz, 3H; 9′-Non). ^{13}C NMR (100 MHz, $[D_1]CDCl_3$, 25°C, TMS): δ= 157.4 (C-2), 145.7 (C-6), 145.3 (C-4), 128.6 (C-3), 125.9 (C-5), 52.1 (NCH_2CH_3), 31.4 (1′-Non), 30.6 (7′-Non), 28.1* (4′-Non), 28.0* (5′,6′-Non), 27.9* (3′-Non), 27.6* (2′-Non), 21.3 (8′-Non), 15.7 (NCH_2CH_3), 12.8 (9′-Non). ESI-HRMS (apex-Qe): m/z (%): 1174 (8) $[(C_{16}H_{28}N)_4\ (Br)_3]^+$, 860 (23) $[(C_{16}H_{28}N)_3\ (Br)_2]^+$, 547.36201 (100) $[(C_{16}H_{28}N)_2\ (Br)]^+$ calcd for 547.36214), 234.22163 (58) $[(C_{16}H_{28}N)]^+$ calcd for 234.22127).

2-Decyl-1-ethylpyridinium bromide (19). Yield 93%. ^{1}H NMR (400 MHz, $[D_1]CDCl_3$, 25°C, TMS): δ=9.79 (dd, *J*(H,H)=1.2 Hz, *J*(H,H)=6.3 Hz, 1H; H-6), 8.84 (td, *J*(H,H)=1.4 Hz, *J*(H,H)=7.9 Hz, 1H; H-4), 8.28 (m, 2H; H-3, H-5), 5.13 (q, *J*(H,H)=7.2 Hz, 2H; NCH_2CH_3), 3.40 (m, 2H; 1′-Dec), 2.03 (m, 2H; 2′-Dec), 1.89 (t, *J*(H,H)=7.2 Hz, 3H; NCH_2CH_3), 1.70 (m, 2H; 3′-Dec), 1.57-1.35 (m, 12H; 4′,5′,6′,7′,8′,9′-Dec), 1.07 (t, *J*(H,H)=6.6 Hz, 3H; 10′-Dec). ^{13}C NMR (100 MHz, $[D_1]CDCl_3$, 25°C, TMS): δ=157.3 (C-2), 145.6 (C-6), 145.3 (C-4), 128.5 (C-3), 126.0 (C-5), 52.2 (NCH_2CH_3), 31.3 (1′-Dec), 30.6 (8′-Dec), 28.2* (4′,5′-Dec), 28.0* (6′,7′-Dec), 27.5* (2′,3′-Dec), 21.4 (9′-Dec), 15.6 (NCH_2CH_3), 12.8 (10′-Dec). ESI-HRMS (apex-Qe): m/z (%): 1230 (11) $[(C_{17}H_{30}N)_4\ (Br)_3]^+$, 902 (30) $[(C_{17}H_{30}N)_3\ (Br)_2]^+$, 575.39344 (100) $[(C_{17}H_{30}N)_2\ (Br)]^+$ calcd for 575.39321), 248.23728 (69) $[(C_{17}H_{30}N)]^+$ calcd for 248.23702).

General procedures for the synthesis of 1-ethyl-2-alkylpyridinium bis(trifluoromethanesulfonyl)imide: An aqueous solution of bis(trifluoromethanesulfonyl)imide lithium salt was added at room temperature, to an equal amount of a stirred aqueous solution of the corresponding 1-ethyl-2-alkylpyridinium bromide and the mixture was stirred for an additional 1 h. Two phases were formed. After addition of dichloromethane (20 mL), the upper aqueous phase was decanted and the lower dichloromethane layer was washed with distilled water (5 x 25 mL). The resulting extracts were dried over anhydrous Na_2SO_4 and evaporated under reduced pressure to afford the desired product. The obtained ILs were dried by heating at 80 °C and stirring under high vacuum (2 x 10^{-1} Pa) for 48 h. All the synthesized 1-ethyl-2-alkylpyridinium bis(trifluoromethanesulfonyl)imide were obtained as slightly yellow liquids.

1,2-Diethylpyridinium bis(trifluoromethanesulfonyl)imide (20). Yield 93%. ^{1}H NMR (400 MHz, [D_1]$CDCl_3$, 25°C, TMS): δ=8.60 (dd, *J*(H,H)=1.2 Hz, *J*(H,H)=6.3 Hz, 1H; H-6), 8.29 (td, *J*(H,H)=1.4 Hz, *J*(H,H)=7.9 Hz, 1H; H-4), 7.81 (m, 1H; H-5), 7.73 (m, 1H; H-3), 4.50 (q, *J*(H,H)=7.3 Hz, 2H; NC$H_2$$CH_3$), 3.05 (q, *J*(H,H)=7.5 Hz, 2H; 1´-Et), 1.50 (t, *J*(H,H)=7.3 Hz, 3H; NCH_2CH_3), 1.35 (t, *J*(H,H)=7.5 Hz, 3H; 2´-Et). ^{13}C NMR (100 MHz, [D_1]$CDCl_3$, 25°C, TMS): δ=158.9 (C-2), 145.0 (C-6), 144.1 (C-4), 127.8 (C-3), 125.5 (C-5), 119.3 (q, *J*(C,F)= 321.3 Hz; $N(SO_2CF_3)_2$), 52.7 (NCH_2CH_3), 25.0 (1´-Et), 15.1 (NCH_2CH_3), 11.3 (2´-Et). ESI-HRMS (apex-Qe): m/z (%): 553 (24) $[(C_9H_{14}N)_2(C_2F_6NO_4S_2) + 1]^+$, 552.14065 (100) $[(C_9H_{14}N)_2(C_2F_6NO_4S_2)]^+$ calcd for 552.14199).

1-Ethyl-2-propylpyridinium bis(trifluoromethanesulfonyl)imide (21). Yield 94%. ^{1}H NMR (400 MHz, [D_1]$CDCl_3$, 25°C, TMS): δ=8.74 (dd, *J*(H,H)=1.4 Hz, *J*(H,H)=6.7 Hz, 1H; H-6), 8.35 (td, *J*(H,H)=1.4 Hz, *J*(H,H)=7.9 Hz, 1H; H-4), 7.85 (m, 2H; H-3, H-5), 4.61 (q, *J*(H,H)=7.3 Hz, 2H; NC$H_2$$CH_3$), 3.05 (m, 2H; 1´-Pr), 1.85 (m, 2H; 2´-Pr), 1.62 (t, *J*(H,H)=7.3 Hz, 3H; NCH_2CH_3), 1.10 (t, *J*(H,H)=7.3 Hz, 3H; 3´-Pr). ^{13}C NMR (100 MHz, [D_1]$CDCl_3$, 25°C, TMS): δ=157.8 (C-2), 144.9 (C-6), 144.4 (C-4), 128.8 (C-3), 125.8 (C-5), 119.41 (q, *J*(C,F)=321.1 Hz; $N(SO_2CF_3)_2$), 52.9 (NCH_2CH_3), 33.5 (1´-Pr), 21.2 (2´-Pr), 15.5 (NCH_2CH_3), 12.9 (3´-Pr). ESI-HRMS (apex-Qe): m/z (%): 581 (24) $[(C_{10}H_{16}N)_2(C_2F_6NO_4S_2) + 1]^+$, 580.17234 (100) $[(C_{10}H_{16}N)_2(C_2F_6NO_4S_2)]^+$ calcd for 580.17329).

2-Butyl-1-ethylpyridinium bis(trifluoromethanesulfonyl)imide (22). Yield 96%. ^{1}H NMR (400 MHz, [D_1]$CDCl_3$, 25°C, TMS): δ=8.70 (dd, *J*(H,H) = 0.8 Hz, *J*(H,H)=6.2 Hz, 1H; H-6), 8.33 (td, *J*(H,H)=1.3 Hz, *J*(H,H)=8.0 Hz, 1H; H-4), 7.83 (m, 2H; H-5, H-3), 4.58 (q, *J*(H,H)=7.3 Hz, 2H; NC$H_2$$CH_3$), 3.05 (m, 2H; 1´-Bu), 1.75 (m, 2H; 2´-Bu), 1.60 (t, *J*(H,H)=7.3 Hz, 3H; NCH_2CH_3), 1.48 (m, 2H; 3´-Bu), 0.96 (t, *J*(H,H)=7.3 Hz, 3H; 4´-Bu). ^{13}C NMR (100 MHz, [D_1]$CDCl_3$, 25°C, TMS): δ=158.2 (C-2), 145.2 (C-6), 144.8 (C-4), 128.9 (C-3), 126.1 (C-5), 119.7 (q, *J*(C,F)=321.3 Hz; $N(SO_2CF_3)_2$), 53.2 (NCH_2CH_3), 32.0 (1´-Bu), 30.2 (2´-Bu), 22.2 (3´-Bu), 15.9 (NCH_2CH_3), 13.4 (4´-Bu). ESI-HRMS (apex-Qe): m/z (%): 609 (23) $[(C_{11}H_{18}N)_2(C_2F_6NO_4S_2) + 1]^+$, 608.20327 (100) $[(C_{11}H_{18}N)_2(C_2F_6NO_4S_2)]^+$ calcd for 608.20459).

1-Ethyl-2-pentylpyridinium bis(trifluoromethanesulfonyl)imide (23). Yield 94%. ^{1}H NMR (400 MHz, [D_1]$CDCl_3$, 25°C, TMS): δ=8.69 (dd, *J*(H,H)=0.8 Hz, *J*(H,H)=6.2 Hz, 1H; H-6), 8.33 (td, *J*(H,H)=1.3 Hz, *J*(H,H)=7.9 Hz, 1H; H-4), 7.82 (m, 2H; H-5, H-3), 4.57 (q, *J*(H,H)=7.3 Hz, 2H; NC$H_2$$CH_3$), 3.04 (m, 2H; 1´-Pen), 1.76 (m, 2H; 2´-Pen), 1.58 (t, *J*(H,H)=7.3 Hz, 3H; NCH_2CH_3), 1.46-1.31 (m, 4H; 3´,4´-Pen), 0.88 (t, *J*(H,H)=7.1 Hz, 3H; 5´-Pen). ^{13}C NMR (100 MHz, [D_1]$CDCl_3$, 25°C, TMS): δ=158.1 (C-2), 145.2 (C-6), 144.8 (C-4), 128.9 (C-3), 126.1 (C-5), 119.6 (q, *J*(C,F)=321.2 Hz; $N(SO_2CF_3)_2$), 53.2 (NCH_2CH_3), 32.1 (1´-Pen), 31.0 (2´-Pen), 27.9 (3´-Pen), 22.0 (4´-Pen), 15.9 (NCH_2CH_3), 13.5 (5´-Pen). ESI-HRMS (apex-Qe): m/z (%): 637 (28) $[(C_{12}H_{20}N)_2(C_2F_6NO_4S_2) + 1]^+$, 636.22024 (100) $[(C_{12}H_{20}N)_2(C_2F_6NO_4S_2)]^+$ calcd for 636.23589).

1-Ethyl-2-hexylpyridinium bis(trifluoromethanesulfonyl)imide (24). Yield 96%. ^{1}H NMR (400 MHz, [D_1]$CDCl_3$, 25°C, TMS): δ=8.68 (dd, *J*(H,H)=0.8 Hz, *J*(H,H)=6.2 Hz, 1H; H-6), 8.32 (td, *J*(H,H)=1.3 Hz, *J*(H,H)=7.9 Hz, 1H; H-4), 7.81 (m, 2H; H-3, H-5), 4.57 (q, *J*(H,H)=7.3 Hz, 2H; NC$H_2$$CH_3$), 3.04 (t, *J*(H,H)=7.9 Hz, 2H; 1´-Hex), 1.75 (m, 2H; 2´-Hex), 1.58 (t, *J*(H,H)=7.3 Hz, 3H; NCH_2CH_3), 1.44 (m, 2H; 3´-Hex), 1.30 (m, 4H; 4´,5´-Hex), 0.85 (t, *J*(H,H)=7.0 Hz, 3H; 6´-Hex). ^{13}C NMR (100 MHz, [D_1]$CDCl_3$, 25°C, TMS): δ=158.1 (C-2), 145.2 (C-6), 144.7 (C-4), 128.9 (C-3), 126.1 (C-5), 119.6 (q, *J*(C,F)=321.3 Hz; $N(SO_2CF_3)_2$), 53.1 (NCH_2CH_3), 32.2 (1´-Hex), 31.1 (4´-Hex), 28.6 (2´-Hex), 28.1 (3´-Hex), 22.2 (5´-Hex), 15.9 (NCH_2CH_3), 13.7 (6´-Hex). ESI-HRMS (apex-Qe): m/z (%): 664.26564 (100) $[(C_{13}H_{22}N)_2(C_2F_6NO_4S_2)]^+$ calcd for 664.26719).

1-Ethyl-2-heptylpyridinium bis(trifluoromethanesulfonyl)imide (25). Yield 97%. ^{1}H NMR (400 MHz, [D_1]$CDCl_3$, 25°C, TMS): δ=8.72 (dd, *J*(H,H)=0.8 Hz, *J*(H,H)=6.2 Hz, 1H; H-6), 8.34 (td, *J*(H,H)=1.3 Hz, *J*(H,H)=8.0 Hz, 1H; H-4), 7.83 (m, 2H; H-3, H-5), 4.59 (q, *J*(H,H)=7.3 Hz, 2H; NC$H_2$$CH_3$), 3.05 (m, 2H; 1´-Hep), 1.77 (m, 2H; 2´-Hep), 1.61 (t, *J*(H,H)=7.3 Hz, 3H; NCH_2CH_3), 1.45 (m, 2H; 3´-Hep), 1.32 (m, 6H; 4´,5´,6´-Hep), 0.86 (t, *J*(H,H)=6.9 Hz, 3H; 7´-Hep). ^{13}C NMR (100 MHz, [D_1]$CDCl_3$, 25°C, TMS): δ=158.1 (C-2), 145.1 (C-6), 144.6 (C-4), 128.9 (C-3), 126.0 (C-5), 119.6 (q, *J*(C,F)=321.4 Hz; $N(SO_2CF_3)_2$), 53.1 (NCH_2CH_3), 32.1 (1´-Hep), 31.2 (5´-Hep), 28.8 (2´-Hep), 28.5* (4´-Hep), 28.1* (3´-Hep), 22.2 (6´-Hep), 15.8 (NCH_2CH_3), 13.7 (7´-Hep). ESI-HRMS (apex-Qe): m/z (%): 693 (26) $[(C_{14}H_{24}N)_2(N(SO_2CF_3)_2) + 1]^+$, 692.29796 (100) $[(C_{14}H_{24}N)_2(C_2F_6NO_4S_2)]^+$ calcd for 692.29849), 206 (47) $[(C_{14}H_{24}N)]^+$.

1-Ethyl-2-octylpyridinium bis(trifluoromethanesulfonyl)imide (26). Yield 98%. ^{1}H NMR (400 MHz, [D_1]$CDCl_3$, 25°C, TMS): δ=8.72 (dd, *J*(H,H)=0.9 Hz, *J*(H,H)=6.2 Hz, 1H; H-6), 8.33 (td, *J*(H,H)=1.3 Hz, *J*(H,H)=8.0 Hz, 1H; H-4), 7.81 (m, 2H; H-3, H-5), 4.58 (q, *J*(H,H)=7.3 Hz, 2H; NC$H_2$$CH_3$), 3.04 (m, 2H; 1´-Oc), 1.75 (m, 2H; 2´-Oc), 1.59 (t, *J*(H,H)=7.3 Hz, 3H; NCH_2CH_3), 1.43 (m, 2H; 3´-Oc), 1.29 (m, 8H; 4´,5´,6´,7´-Oc), 0.84 (t, *J*(H,H)=6.8 Hz, 3H; 8´-Oc). ^{13}C NMR (100 MHz, [D_1]$CDCl_3$, 25°C, TMS): δ=158.0 (C-2), 145.1 (C-6), 144.6 (C-4), 128.8 (C-3), 125.9 (C-5), 119.5 (q, *J*(C,F)=321.3 Hz; $N(SO_2CF_3)_2$), 53.0 (NCH_2CH_3), 32.0 (1´-Oc), 31.4 (6´-Oc), 28.8* (2´-Oc), 28.8* (4´-Oc), 28.7 (3´-Oc), 28.1 (5´-Oc), 22.3 (7´-Oc), 15.7 (NCH_2CH_3), 13.7 (8´-Oc). ESI-HRMS (apex-Qe): m/z (%): 720 (11) $[(C_{15}H_{26}N)_2(C_2F_6NO_4S_2)]^+$, 220.20581 (100) $[(C_{14}H_{24}N)]^+$ calcd for 220.20598).

1-Ethyl-2-nonylpyridinium bis(trifluoromethanesulfonyl)imide (27). Yield 99%. ^{1}H NMR (400 MHz, [D_1]$CDCl_3$, 25°C, TMS): δ=8.75 (dd, *J*(H,H)=1.2 Hz, *J*(H,H)=6.3 Hz, 1H; H-6), 8.35 (td, *J*(H,H)=1.4 Hz, *J*(H,H)=7.9 Hz, 1H; H-4), 7.85 (m, 2H; H-3, H-5), 4.61 (q, *J*(H,H)=7.3 Hz, 2H; NC$H_2$$CH_3$), 3.06 (m, 2H; 1´-Non), 1.75

(m, 2H; 2´-Non), 1.62 (t, *J*(H,H)=7.3 Hz, 3H; NCH_2CH_3), 1.45 (m, 2H; 3´-Non), 1.37-1.18 (m, 10H; 4´,5´,6´,7´,8´-Non), 0.86 (t, *J*(H,H)=6.9 Hz, 3H; 9´-Non). ^{13}C NMR (100 MHz, $[D_1]CDCl_3$, 25°C, TMS): δ= 158.7 (C-2), 145.6 (C-6), 145.0 (C-4), 129.2 (C-3), 126.3 (C-5), 119.9 (q, *J*(C,F)=321.3 Hz; $N(SO_2CF_3)_2$), 52.9 (NCH_2CH_3), 31.8 (1´-Non), 31.3 (7´-Non), 28.8* (4´-Non), 28.7* (5´-Non), 28.6 (3´,6´-Non), 27.9* (2´-Non), 22.1 (8´-Non), 15.4 (NCH_2CH_3), 13.4 (9´-Non). ESI-HRMS (apex-Qe): m/z (%): 748.36100 (100) ($[(C_{16}H_{28}N)_2(C_2F_6NO_4S_2)]^+$ calcd for 748.36109).

2-Decyl-1-ethylpyridinium bis(trifluoromethanesulfonyl)imide (28). Yield 98%. ^{1}H NMR (400 MHz, $[D_1]CDCl_3$, 25°C, TMS): δ=8.64 (dd, *J*(H,H)=1.2 Hz, *J*(H,H)=6.3 Hz, 1H; H-6), 8.30 (td, *J*(H,H)=1.4 Hz, *J*(H,H)=7.9 Hz, 1H; H-4), 7.77 (m, 2H; H-3, H-5), 4.54 (q, *J*(H,H)=7.2 Hz, 2H; NCH_2CH_3), 3.00 (m, 2H; 1´-Dec), 1.71 (m, 2H; 2´-Dec), 1.55 (t, *J*(H,H)=7.2 Hz, 3H; NCH_2CH_3), 1.39 (m, 2H; 3´-Dec), 1.28-1.09 (m, 12H; 4´,5´,6´,7´,8´,9´-Dec), 0.79 (t, *J*(H,H)=6.6 Hz, 3H; 10´-Dec). ^{13}C NMR (100 MHz, $[D_1]CDCl_3$, 25°C, TMS): δ=158.7 (C-2), 145.6 (C-6), 145.1 (C-4), 129.3 (C-3), 126.3 (C-5), 119.9 (q, *J*(C,F)=321.3 Hz; $N(SO_2CF_3)_2$), 53.0 (NCH_2CH_3), 31.9 (1´-Dec), 31.4 (8´-Dec), 29.0* (4´-Dec), 28.9* (5´-Dec), 28.8* (6´-Dec), 28.7* (7´-Dec), 28.6* (3´-Dec), 27.9* (2´-Dec), 22.1 (9´-Dec), 15.4 (NCH_2CH_3), 13.5 (10´-Dec). ESI-HRMS (apex-Qe): m/z (%): 776.39227 (100) ($[(C_{17}H_{30}N)_2(C_2F_6NO_4S_2)]^+$ calcd for 776.39239), 248.23713 (56) ($[(C_{17}H_{30}N)]^+$ calcd for 248.23702).

Vapor Pressure Measurements

Purification: Before the vapor pressure measurements, the ionic liquids were dried under reduced pressure (< 10 Pa) and stirred constantly for a minimum of 48 h at 323 K, in order to reduce the presence of water or other volatile contents. Afterwards, an in situ purification of the ionic liquids was performed using the Knudsen effusion installation, at high vacuum (1×10^{-7} Pa).

Quartz crystal microbalance Knudsen effusion apparatus: The vapor pressures of the ionic liquids were measured as a function of temperature using a new Knudsen effusion method combined with a quartz crystal microbalance,[55] Basically, this apparatus results on the combination of the Knudsen effusion technique and quartz crystal microbalance. In a typical KEQCM experiment, the measurement of the equilibrium vapor pressure at a given temperature, *T*, is achieved by the vapor effusion through the orifice of a effusion cell and condensation of a fraction of the vapor on the surface of the cooled quartz crystal, placed above the effusion cell. This apparatus comprises two mass loss detection techniques, gravimetric and quartz crystal microbalance: the weighed mass of the effusion cell before and after the respective experiment, and the change of the crystal's resonant frequency as the vapor condense on its surface. The combination of these two mass loss detection techniques presents several advantages, such as, small effusion times, small sample size and real time monitoring of the effusion experiment. The instrument enables the measurement of vapor pressures from 0.02 Pa up to 1 Pa and the temperature is controlled within a temperature fluctuation of $\pm(5\times10^{-3})$ K, measured with a resolution better than 1×10–3 K and along the working temperature range, the overall uncertainty is better than $\pm(2\times10^{-2})$ K. The vapor pressure data obtained with this apparatus for the ionic liquid have a typical pressure dependent uncertainty of (1 to 5) %.[56] The relative atomic masses used were those recommended by the IUPAC Commission in 2007.[93]

Electrospray Tandem Mass Spectrometry (ESI-MS-MS)

Electrospray ionization mass spectra (ESI-MS) with a Micromass Q-Tof 2 (Micromass, Manchester, UK), operating in the positive ion mode, equipped with a Z-spray source was used. Source and desolvation temperatures were 353 K and 373 K, respectively. Ionic liquids solutions in methanol, at concentrations circa to 10^{-4} mol·dm^{-3}, were introduced at a 10 μL·min^{-1} flow rate. The capillary and the cone voltage were 2600V (or 3000 V) and 30 V, respectively. Nitrogen was used as nebulization gas and argon as collision gas. This method has already proved to be an adequate strategy in the study of the relative cation-anion interaction strength in ILs.[62] Further details can be found elsewhere. [62] ESI-MS-MS spectra were acquired by selecting the precursor ion with the quadrupole, and performing collisions with argon at variable energies in the hexapole. The laboratory frame collision energy (E_{Lab}) can be changed and is reflected by a variation in the collision energy fraction that is actually converted to the ions' internal energy. The variable collisions energies in the ESI-MS-MS spectra are taken from the relative abundances of precursor and fragment ions, whereas the energy values corresponding to a relative abundance of the precursor ion of 50% ($E_{Lab,1/2}$) are here used as a measure of the relative dissociation energy. In this inelastic collision of the projectile ion with the target neutral, the total available energy for conversion of translational (or kinetic) to internal (or vibrational) energy of the projectile ion is the center of mass energy (E_{cm}), which can be calculated from E_{Lab}, and from the masses of the neutral target and precursor ion. The calculated dissociation energies from the experimental E_{Lab} values represent the energy necessary to separate a cation from the neutral IL in the gas phase and, as such, can be considered a good approximation to the cation-anion relative interaction energy. Triplicate measurements were performed for each selected precursor ion and standard deviations varying between 0.3% and 5% were obtained.

Supporting Information: The experimental vapor pressure results at different temperatures, the graphic representations of the thermodynamic properties of vaporization at T = 298.15 K as a function of the total number of carbon atoms in the two alkyl side chains of the cation, N, as well the ^{13}C NMR spectrum are presented as supporting information.

Acknowledgements

The authors are grateful to the Ministerio de Economía y Competitividad of Spain (Ref. DPI2012-38841-C02-02), to the Xunta de Galicia (project 2012/184) and the Galician Network on Ionic Liquids REGALIs (CN 2012/120) for financial support. Thanks are due to Fundação para a Ciência e Tecnologia (FCT), Lisbon, Portugal and to FEDER for financial support to Centro de Investigação em Química, University of Porto through the project Pest-C/QUI/UI0081/2011. Marisa A. A. Rocha acknowledges the financial support from FCT and the European Social Fund (ESF) under the Community Support Framework (CSF) for the award of a Ph.D. Research Grant, SFRH/BD/60513/2009.

Received: ((will be filled in by the editorial staff))
Revised: ((will be filled in by the editorial staff))
Published online: ((will be filled in by the editorial staff))

1. S. M. Urahata and M. C. C. Ribeiro, *J. Chem. Phys.*, 2004, **120**, 1855–63.
2. Y. Wang and G. A. Voth, *J. Am. Chem. Soc.*, 2005, **127**, 12192–3.
3. S. Izvekov and G. A. Voth, *J. Chem. Phys.*, 2005, **123**, 134105.
4. J. N. A. Canongia Lopes and A. A. H. Pádua, *J. Phys. Chem. B*, 2006, **110**, 3330–5.
5. K. Shimizu, M. F. Costa Gomes, A. A. H. Pádua, L. P. N. Rebelo, and J. N. Canongia Lopes, *J. Mol. Struct. THEOCHEM*, 2010, **946**, 70–76.
6. M. F. C. Gomes, J. N. C. Lopes, and A. A. H. Padua, *Top. Curr. Chem.*, 2010, **290**, 161–83.
7. A. Triolo, O. Russina, H.-J. Bleif, and E. Di Cola, *J. Phys. Chem. B*, 2007, **111**, 4641–4.
8. O. Russina, A. Triolo, L. Gontrani, R. Caminiti, D. Xiao, L. G. Hines Jr, R. A. Bartsch, E. L. Quitevis, N. Pleckhova, and K. R. Seddon, *J. Phys. Condens. Matter*, 2009, **21**, 424121.
9. A. Triolo, O. Russina, B. Fazio, G. B. Appetecchi, M. Carewska, and S. Passerini, *J. Chem. Phys.*, 2009, **130**, 164521.
10. C. Hardacre, J. D. Holbrey, S. E. J. McMath, D. T. Bowron, and A. K. Soper, *J. Chem. Phys.*, 2003, **118**, 273.
11. C. Hardacre, S. E. J. McMath, M. Nieuwenhuyzen, D. T. Bowron, and A. K. Soper, *J. Phys. Condens. Matter*, 2003, **15**, S159–S166.
12. A. Triolo, A. Mandanici, O. Russina, V. Rodriguez-Mora, M. Cutroni, C. Hardacre, M. Nieuwenhuyzen, H.-J. Bleif, L. Keller, and M. A. Ramos, *J. Phys. Chem. B*, 2006, **110**, 21357–64.
13. K. Fujii, T. Fujimori, T. Takamuku, R. Kanzaki, Y. Umebayashi, and S.-I. Ishiguro, *J. Phys. Chem. B*, 2006, **110**, 8179–83.
14. C. M. Burba, J. Janzen, E. D. Butson, and G. L. Coltrain, *J. Phys. Chem. B*, 2013, **117**, 8814–20.
15. O. Russina, A. Triolo, L. Gontrani, and R. Caminiti, *J. Phys. Chem. Lett.*, 2012, **3**, 27–33.
16. K. Shimizu, C. E. S. Bernardes, and J. N. Canongia Lopes, *J. Phys. Chem. B*, 2014, **118**, 567–76.
17. K. N. Marsh, A. Deev, A. C.-T. Wu, E. Tran, and A. Klamt, *Korean J. Chem. Eng.*, 2002, **19**, 357–362.
18. S. Zhang, N. Sun, X. He, X. Lu, and X. Zhang, *J. Phys. Chem. Ref. Data*, 2006, **35**, 1475.
19. J. M. S. S. Esperança, J. N. Canongia Lopes, M. Tariq, L. M. N. B. F. Santos, J. W. Magee, and L. P. N. Rebelo, *J. Chem. Eng. Data*, 2010, **55**, 3–12.
20. H. Liu, E. Maginn, A. E. Visser, N. J. Bridges, and E. B. Fox, *Ind. Eng. Chem. Res.*, 2012, **51**, 7242–7254.
21. R. G. Seoane, S. Corderí, E. Gómez, N. Calvar, E. J. González, E. A. Macedo, and Á. Domínguez, *Ind. Eng. Chem. Res.*, 2012, **51**, 2492–2504.
22. S. Aparicio, M. Atilhan, and F. Karadas, *Ind. Eng. Chem. Res.*, 2010, **49**, 9580–9595.
23. Y. U. Paulechka, *J. Phys. Chem. Ref. Data*, 2010, **39**, 033108.
24. W. Zheng, A. Mohammed, L. G. Hines, D. Xiao, O. J. Martinez, R. A. Bartsch, S. L. Simon, O. Russina, A. Triolo, and E. L. Quitevis, *J. Phys. Chem. B*, 2011, **115**, 6572–84.
25. S. Stevanovic and M. F. Costa Gomes, *J. Chem. Thermodyn.*, 2013, **59**, 65–71.
26. D. Rooney, J. Jacquemin, and R. Gardas, *Top. Curr. Chem.*, 2010, **290**, 185–212.
27. J. A. P. Coutinho, P. J. Carvalho, and N. M. C. Oliveira, *RSC Adv.*, 2012, **2**, 7322.
28. R. L. Gardas and J. A. P. Coutinho, *AIChE J.*, 2009, **55**, 1274–1290.
29. M. J. Earle, J. M. S. S. Esperança, M. A. Gilea, J. N. C. Lopes, L. P. N. Rebelo, J. W. Magee, K. R. Seddon, and J. A. Widegren, *Nature*, 2006, **439**, 831–4.
30. J. Albert and K. Müller, *Ind. Eng. Chem. Res.*, 2014, 141022093335006.
31. Y. U. Paulechka, D. H. Zaitsau, G. J. Kabo, and A. A. Strechan, *Thermochim. Acta*, 2005, **439**, 158–160.
32. D. H. Zaitsau, G. J. Kabo, A. A. Strechan, Y. U. Paulechka, A. Tschersich, S. P. Verevkin, and A. Heintz, *J. Phys. Chem. A*, 2006, **110**, 7303–6.
33. L. M. N. B. F. Santos, J. N. C. Lopes, J. A. P. Coutinho, J. M. S. S. Esperança, L. R. Gomes, I. M. Marrucho, and L. P. N. Rebelo, *J. Am. Chem. Soc.*, 2007, **129**, 284–5.
34. D. Strasser, F. Goulay, M. S. Kelkar, E. J. Maginn, and S. R. Leone, *J. Phys. Chem. A*, 2007, **111**, 3191–5.
35. V. N. Emel'yanenko, S. P. Verevkin, A. Heintz, J.-A. Corfield, A. Deyko, K. R. J. Lovelock, P. Licence, and R. G. Jones, *J. Phys. Chem. B*, 2008, **112**, 11734–42.
36. J. P. Armstrong, C. Hurst, R. G. Jones, P. Licence, K. R. J. Lovelock, C. J. Satterley, and I. J. Villar-Garcia, *Phys. Chem. Chem. Phys.*, 2007, **9**, 982–90.
37. K. R. J. Lovelock, A. Deyko, J.-A. Corfield, P. N. Gooden, P. Licence, and R. G. Jones, *Chemphyschem*, 2009, **10**, 337–40.
38. J. P. Leal, J. M. S. S. Esperança, M. E. M. da Piedade, J. N. C. Lopes, L. P. N. Rebelo, and K. R. Seddon, *J. Phys. Chem. A*, 2007, **111**, 6176–82.
39. J. P. Leal, M. E. M. da Piedade, J. N. Canongia Lopes, A. A. Tomaszowska, J. M. S. S. Esperança, L. P. N. Rebelo, and K. R. Seddon, *J. Phys. Chem. B*, 2009, **113**, 3491–8.
40. S. D. Chambreau, G. L. Vaghjiani, A. To, C. Koh, D. Strasser, O. Kostko, and S. R. Leone, *J. Phys. Chem. B*, 2010, **114**, 1361–7.
41. A. Deyko, K. R. J. Lovelock, J.-A. Corfield, A. W. Taylor, P. N. Gooden, I. J. Villar-Garcia, P. Licence, R. G. Jones, V. G. Krasovskiy, E. A. Chernikova, and L. M. Kustov, *Phys. Chem. Chem. Phys.*, 2009, **11**, 8544–55.
42. S. P. Verevkin, V. N. Emel'yanenko, D. H. Zaitsau, R. V Ralys, and C. Schick, *J. Phys. Chem. B*, 2012, **116**, 4276–85.
43. S. P. Verevkin, D. H. Zaitsau, V. N. Emel'yanenko, R. V. Ralys, A. V. Yermalayeu, and C. Schick, *J. Chem. Thermodyn.*, 2012, **54**, 433–437.
44. K. Fumino, A. Wulf, S. P. Verevkin, A. Heintz, and R. Ludwig, *Chemphyschem*, 2010, **11**, 1623–6.
45. S. P. Verevkin, D. H. Zaitsau, V. N. Emel'yanenko, A. V Yermalayeu, C. Schick, H. Liu, E. J. Maginn, S. Bulut, I. Krossing, and R. Kalb, *J. Phys. Chem. B*, 2013, **117**, 6473–86.
46. D. H. Zaitsau, A. V. Yermalayeu, V. N. Emel'yanenko, S. P. Verevkin, U. Welz-Biermann, and T. Schubert, *Sci. China Chem.*, 2012, **55**, 1525–1531.
47. T. Köddermann, D. Paschek, and R. Ludwig, *Chemphyschem*, 2008, **9**, 549–55.
48. R. Ludwig, *Phys. Chem. Chem. Phys.*, 2008, **10**, 4333–9.
49. F. Dommert, K. Wendler, R. Berger, L. Delle Site, and C. Holm, *ChemPhysChem*, 2012, **13**, 1625–1637.
50. M. A. A. Rocha, C. F. R. A. C. Lima, L. R. Gomes, B. Schröder, J. A. P. Coutinho, I. M. Marrucho, J. M. S. S. Esperança, L. P. N. Rebelo, K. Shimizu, J. N. C. Lopes, and L. M. N. B. F. Santos, *J. Phys. Chem. B*, 2011, **115**, 10919–26.
51. M. A. A. Rocha, J. A. P. Coutinho, and L. M. N. B. F. Santos, *J. Phys. Chem. B*, 2012, **116**, 10922–7.
52. M. A. A. Rocha, C. M. S. S. Neves, M. G. Freire, O. Russina, A. Triolo, J. A. P. Coutinho, and L. M. N. B. F. Santos, *J. Phys. Chem. B*, 2013, **117**, 10889–10897.
53. M. A. A. Rocha and L. M. N. B. F. Santos, *Chem. Phys. Lett.*, 2013, **585**, 59–62.

54. M. A. A. Rocha, F. M. S. Ribeiro, A. I. M. C. L. Ferreira, J. A. P. Coutinho, and L. M. N. B. F. Santos, *J. Mol. Liq.*, 2013, **188**, 196–202.
55. M. A. A. Rocha, J. A. P. Coutinho, and L. M. N. B. F. Santos, *J. Chem. Phys.*, 2014.
56. L. M. N. B. F. Santos, L. M. S. S. Lima, C. F. R. A. C. Lima, F. D. Magalhães, M. C. Torres, B. Schröder, and M. A. V. Ribeiro da Silva, *J. Chem. Thermodyn.*, 2011, **43**, 834–843.
57. M. A. A. Rocha, J. A. P. Coutinho, and L. M. N. B. F. Santos, *J. Chem. Phys.*, 2013, **139**, 104502.
58. P. Verdía, E. J. González, B. Rodríguez-Cabo, and E. Tojo, *Green Chem.*, 2011, **13**, 2768.
59. H. Gao, M. Luo, J. Xing, Y. Wu, Y. Li, W. Li, Q. Liu, and H. Liu, *Ind. Eng. Chem. Res.*, 2008, **47**, 8384–8388.
60. C. Cadena, Q. Zhao, R. Q. Snurr, and E. J. Maginn, *J. Phys. Chem. B*, 2006, **110**, 2821–32.
61. M. B. Oliveira, F. Llovell, J. A. P. Coutinho, and L. F. Vega, *J. Phys. Chem. B*, 2012, **116**, 9089–100.
62. A. M. Fernandes, M. A. A. Rocha, M. G. Freire, I. M. Marrucho, J. A. P. Coutinho, and L. M. N. B. F. Santos, *J. Phys. Chem. B*, 2011, **115**, 4033–41.
63. M. García-Mardones, I. Bandrés, M. C. López, I. Gascón, and C. Lafuente, *J. Solution Chem.*, 2012, **41**, 1836–1852.
64. W. Xu, L.-M. Wang, R. A. Nieman, and C. A. Angell, *J. Phys. Chem. B*, 2003, **107**, 11749–11756.
65. Y. Yoshida, O. Baba, and G. Saito, *J. Phys. Chem. B*, 2007, **111**, 4742–4749.
66. M. A. A. Rocha, Universidade do Porto, 2013.
67. E. C. W. Clarke and D. N. Glew, *Trans. Faraday Soc.*, 1966, **62**, 539.
68. P. J. Mohr, B. N. Taylor, and D. B. Newell, *Rev. Mod. Phys.*, 2012, **84**, 1527–1605.
69. D. H. Zaitsau, A. V. Yermalayeu, V. N. Emel'yanenko, A. Heintz, S. P. Verevkin, C. Schick, S. Berdzinski, and V. Strehmel, *J. Mol. Liq.*, 2014, **192**, 171–176.
70. V. N. Emel'yanenko, S. P. Verevkin, and A. Heintz, *J. Am. Chem. Soc.*, 2007, **129**, 3930–7.
71. S. P. Verevkin, V. N. Emel'yanenko, D. H. Zaitsau, A. Heintz, C. D. Muzny, and M. Frenkel, *Phys. Chem. Chem. Phys.*, 2010, **12**, 14994–5000.
72. S. P. Verevkin, D. H. Zaitsau, V. N. Emelyanenko, and A. Heintz, *J. Phys. Chem. B*, 2011, **115**, 12889–95.
73. D. H. Zaitsau, S. P. Verevkin, V. N. Emel'yanenko, and A. Heintz, *Chemphyschem*, 2011, **12**, 3609–13.
74. S. P. Verevkin, R. V. Ralys, D. H. Zaitsau, V. N. Emel'yanenko, and C. Schick, *Thermochim. Acta*, 2012, **538**, 55–62.
75. S. P. Verevkin, D. H. Zaitsau, V. N. Emel'yanenko, A. V Yermalayeu, C. Schick, H. Liu, E. J. Maginn, S. Bulut, I. Krossing, and R. Kalb, *J. Phys. Chem. B*, 2013, **117**, 6473–86.
76. M. A. A. Rocha, F. M. S. Ribeiro, B. Schröder, J. A. P. Coutinho, and L. M. N. B. F. Santos, *J. Chem. Thermodyn.*, 2014, **68**, 317–321.
77. Y. U. Paulechka, G. J. Kabo, and V. N. Emel'yanenko, *J. Phys. Chem. B*, 2008, **112**, 15708–17.
78. A. V. Blokhin, Y. U. Paulechka, and G. J. Kabo, *J. Chem. Eng. Data*, 2006, **51**, 1377–1388.
79. A. V Blokhin, Y. U. Paulechka, A. A. Strechan, and G. J. Kabo, *J. Phys. Chem. B*, 2008, **112**, 4357–64.
80. Y. U. Paulechka, A. V. Blokhin, G. J. Kabo, and A. A. Strechan, *J. Chem. Thermodyn.*, 2007, **39**, 866–877.
81. K. S. Rane and J. R. Errington, *J. Phys. Chem. B*, 2014, **118**, 8734–43.
82. K. Růžička and V. Majer, *J. Phys. Chem. Ref. Data*, 1994, **23**, 1.
83. D. Matulis, *Biophys. Chem.*, 2001, **93**, 67–82.
84. J. S. Chickos and W. Hanshaw, *J. Chem. Eng. Data*, 2004, **49**, 77–85.
85. C. Smit, M. W. Fraaije, and A. J. Minnaard, *J. Org. Chem.*, 2008, **73**, 9482–5.
86. X. Chen, C. E. Goodhue, and J.-Q. Yu, *J. Am. Chem. Soc.*, 2006, **128**, 12634–5.
87. K. Tamao, S. Kodama, I. Nakajima, M. Kumada, A. Minato, and K. Suzuki, *Tetrahedron*, 1982, **38**, 3347–3354.
88. H. B. A. B. De Haan, *Fundamentals of Industrial Separations*, .
89. J. W. Tilley and S. Zawoiski, *J. Org. Chem.*, 1988, **53**, 386–390.
90. J.-L. Zhu, Y.-L. Su, Y.-H. Chang, I.-C. Chen, and C.-C. Liao, *Heterocycles*, 2009, **78**, 369.
91. I. Kondolff, H. Doucet, and M. Santelli, *Tetrahedron*, 2004, **60**, 3813–3818.
92. L. Vandromme, H.-U. Reißig, S. Gröper, and J. P. Rabe, *European J. Org. Chem.*, 2008, **2008**, 2049–2055.
93. M. E. Wieser and M. Berglund, *Pure Appl. Chem.*, 2009, **81**, 2131–2156.

PCCP

RSCPublishing

ARTICLE